Chapter 2

Materials and Methods

2. Materials and Methods

2.1. Materials

CBD, was supplied as a gift from GW Pharma, UK (Figure 2.1.). Cisplatin, quercetin and acetate were obtained from Sigma, UK. All other reagents were obtained from their respective supplier (see below).

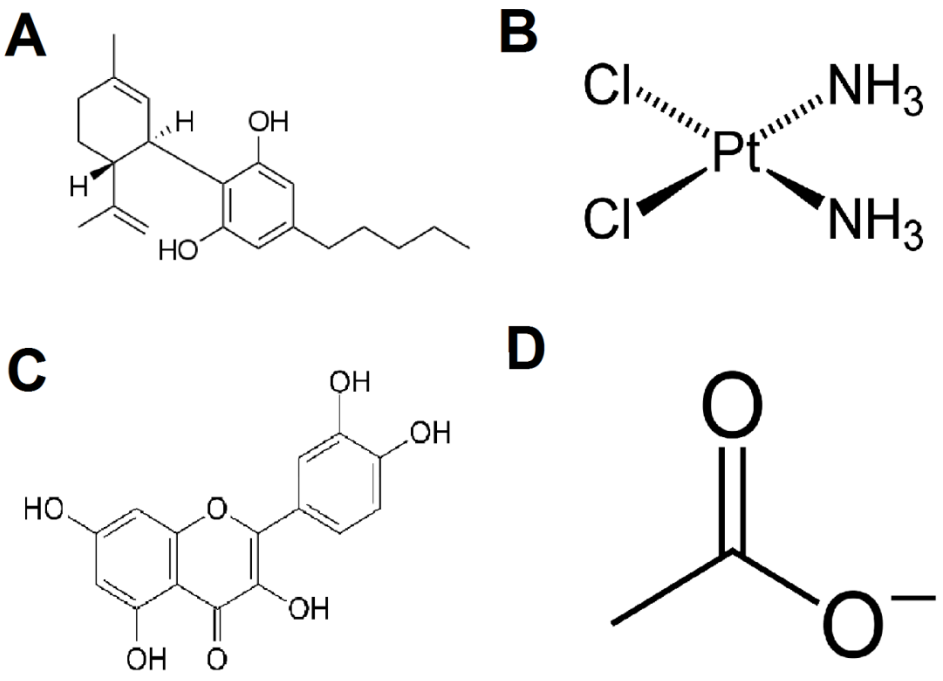

Figure 2.1. Molecular structures of agents used.
The chemical structures of **(A)** CBD, **(B)** cisplatin, **(C)** quercetin and **(D)** acetate.

2.2. Drug preparation for experiments

2.2.1. Cannabidiol, CBD preparation

CBD was prepared fortnightly as a stock ranging from 10 mM to 100 μM in dimethylsulphoxide (DMSO) and water (1:4). The stock solution was kept at 4°C in a glass vial. Treatment dilutions were made up fresh on the day in the required media and never exceeded a DMSO concentration of 1%.

2.2.2. Cisplatin preparation

Cisplatin was prepared as directed from the supplier (Sigma, UK) by diluting in sterile water. Stocks of 10 mM were prepared fresh fortnightly and kept in a glass vial. Dilutions for treatment were made in the corresponding required media fresh on the day of treatment.

2.2.3. Preparation of quercetin

Quercetin was prepared according to Sigma's conditions with DMSO. Fresh stock was made when required at a concentration of 100 mM with the corresponding required media. Dilutions of quercetin never exceeded a DMSO concentration of 1%.

2.2.4. Acetate preparation

Sodium acetate was prepared according to Sigma, UK with sterile water. Fresh stock was prepared when required and filtered using a 0.22 µm syringe filter prior to use into a glass vial. Stock concentrations of 100 mM were prepared and diluted accordingly in the corresponding required media.

2.3. Cells used in the studies

Various different human cancer and control cells were used throughout this study and were obtained from several different sources. The breast cancer cell line MDA-MB231 (invasive, metastatic, oestrogen receptor negative (ER-)) was obtained from Dr. T. Kalber (MRC CSC). Control human breast cell line, MCF10A (epithelial mammary tissue), breast cancer cell line, MCF7 (invasive, metastatic, oestrogen receptor positive (ER+)) and colon cancer cell line, HT29 (colorectal epithelial adenocarcinoma, CD4-) were donated by Dr. N. Haiji, (Imperial College London). HepG2 a liver cancer cell line (epithelial hepatocellular carcinoma, non-tumourogenic) was donated by Dr. L. Brody (MRC CSC). Lung cancer cell line, A549 (hypotriploid human cell line) and Rho0 (Complex I and complex IV of the mitochondria knocked out in A549 cells) was gifted by Dr. N. Navaratnam (MRC CSC).

2.4. Cell culture conditions

Human breast cancer cell line, MDA-MB231, were grown in Media 1: Dulbecco's Modified Eagle Media (DMEM) (Sigma, UK) with 10% Fetal Bovine Serum (FBS)

(Sigma, UK), 1% L-Glutamine (Invitrogen, UK) and 1% Penicillin/Streptomycin (P/S) solution (Invitrogen, UK) (Table 2.1.). Control cells, MCF10A, were grown in Media 2: DMEM:F12 (Life Sciences, UK) supplemented with 5% horse serum (Sigma, UK), 1% P/S, 20 ng/mL epidermal growth factor (EGF) (Sigma, UK), 0.5 mg/mL hydrocortisone (Sigma, UK), 100 ng/mL cholera toxin (Sigma, UK), 10 µg/mL insulin (Sigma, UK). Colon cancer cells HT29 are an epithelial colorectal adenocarcinoma that was cultured using media 1. Lung cancer cells, A549 are a basal epithelial adenocarcinoma cell line and media 1 supplemented with 0.05% uridine was used in all experiments. Liver cancer cells HepG2 are a hepatocellular carcinoma that was cultured using media 1. Human breast cancer cells line MCF7 cells were grown in media 3: Essential Minimum Eagle Media (EMEM) (Sigma, UK), with 10% FBS (Sigma, UK), 1% L-Glutamine (Invitrogen, UK) and 1% P/S solution (Invitrogen, UK). Mitochondrial altered cells, Rho0, were maintained with media 1. All cells were maintained at 37°C in a humidified 5% carbon dioxide (CO_2) atmosphere. Quality control of the cells was maintained by periodic mycoplasma testing.

Table 2.1. Cell Culture Conditions. Cell name and type that was used for the consequent experiments and the media that the cells were maintained under.

Cell Name	Cell Type	Human	Culture Conditions
MDA-MB231	Breast Cancer (ER-)	Yes	Media 1
MCF10A	Breast non-cancer	Yes	Media 2
MCF7	Breast Cancer (ER+)	Yes	Media 3
HT29	Colon Cancer	Yes	Media 1
HepG2	Liver Cancer	Yes	Media 1
A549	Lung Cancer	Yes	Media 1 + 0.05% Uridine
Rho0	Mitochondria altered	Yes	Media 1

Media 1: DMEM (Sigma, UK) with 10% FBS (Sigma, UK), 1% L-Glutamine (Invitrogen, UK) and 1% P/S solution (Invitrogen, UK).
Media 2: DMEM:F12 (Life Sciences, UK) supplemented with 5% horse serum (Sigma, UK), 1% P/S, 20 ng/mL EGF (Sigma UK), 0.5 mg/mL hydrocortisone (Sigma, UK), 100 ng/mL cholera toxin (Sigma, UK), 10 µg/mL insulin (Sigma, UK).
Media 3: EMEM (Sigma, UK), with 10% FBS (Sigma, UK), 1% L-Glutamine (Invitrogen, UK) and 1% P/S solution (Invitrogen, UK).

2.5. Cell maintenance and treatment preparation

Cells lines were maintained in the conditions described in 2.4 in either T175 or T75 flasks (Nunc, USA) and grown as a monolayer. Cells were maintained every 3-5 days never exceeding 20 passages. Once the cells were approximately 80% confluent, they were harvested for treatment or passaged to a fresh flask for maintenance. To prepare the cells for treatment the media was removed and the flasks washed in phosphate buffered saline (PBS). TripLE (Sigma, UK) was added at 10% of the starting volume and left for approximately 5 minutes at 37°C in a 5% CO_2 chamber. The TripLE was inactivated with the addition of the appropriate corresponding media to a known concentration. This was then removed and centrifuged at 1200 revolutions per minute (RPM) for 3 minutes at room temperature. The supernatant was removed and the cell pellet was resuspended with appropriate media to a known volume. A 1:1 ratio of trypan blue:cells was prepared and loaded onto a haemocytometer to be counted. The cells were then either seeded for treatment or placed in a fresh flask for maintenance.

2.6. Experimental treatment conditions

2.6.1. Acute (1 hour) cannabidiol, CBD, treatment

Cell media was removed from the incubation chamber 24 hours after seeding. The cells were washed with PBS and consequently incubated with prepared dilutions of CBD (0 μM-5 μM) for 1 hour.

2.6.2. Chronic (24 hour) cannabidiol, CBD, treatment

Cell media was removed from the incubation chamber 24 hours after seeding. The cells were washed with PBS and consequently incubated with prepared dilutions of CBD (0 μM-5 μM), sodium acetate (1mM) or quercetin (40 μM) for 24 hours.

2.6.3. Cisplatin treatment conditions

Cells were allowed to adhere in the incubation chamber for 24 hours. The media was then removed, cells washed with PBS and treated with a range of cisplatin (0 μM-150 μM) dissolved in cell culture media for 24 hours.

2.6.4. Combination treatment conditions

After allowing the cells to adhere to the incubation chamber for 24 hours prior to treatment. The cells were washed with PBS and treated with a combination of CBD (1 μM) and cisplatin (100 μM) for 24 hours that was freshly prepared prior to each treatment.

2.6.5. “Priming” treatment method

Cells were seeded in an incubation chamber that corresponded to the desired experiment to be carried out and after 24 hours the media was removed and replaced with a “priming” agent after washing with PBS. The “priming” agent was CBD (1 μM),

quercetin (40 μM) or sodium acetate (1 mM) for 24 hours (Figure 2.2.). After this incubation period the media was removed and the chamber was washed with PBS gently before being replaced with media supplemented with cisplatin (50 μM or 100 μM) for a further 24 hours. Experiments were carried out after this 48 hour incubation.

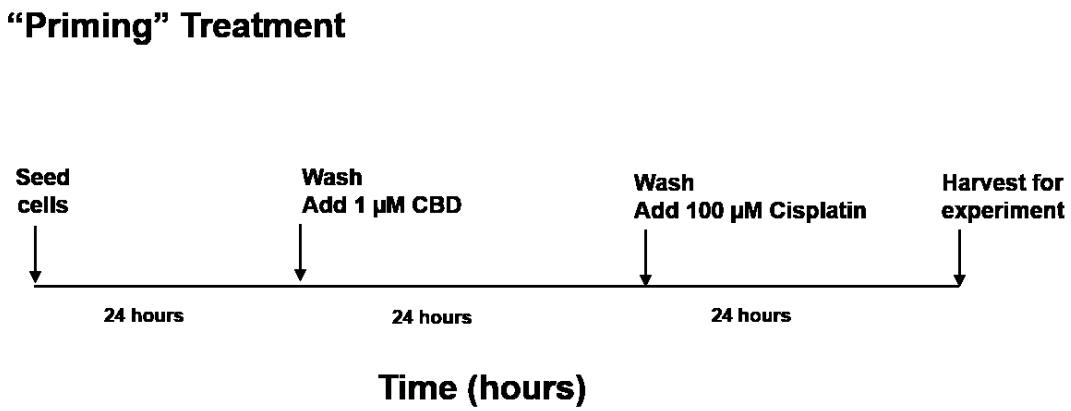

Figure 2.2. "Priming" treatment schematic.
The cells are seeded for 24 hours prior to treatment. The cells are washed and treated with 1 μM CBD (the "priming" agent) for 24 hours. The cells are then washed and treated with 100 μM cisplatin for a further 24 hours. The cells are then ready for experimentation.

2.7. Cell viability assessment

2.7.1. Fluorescence-activated cell sorting (FACS) analysis

After treatment with CBD, the media was collected. The cells were washed with PBS which was also collected into the same tube. The cells were collected also by incubating with 10% TripLE into the same tube. The solution was pelleted by centrifugation at 1200 RPM for 5 minutes to collect both the live and dead cell populations. The pellet was resuspended in PBS and aliquoted into fresh round-bottom tubes. For cell viability and permeability assessment 3,3'-diethyloxadicarbocyanine Iodide (DiOC) /Propidium Iodide (PI) was added to the samples by suspending the pellet in freshly prepared warm PBS, 3 μM PI and 0.04 μM DiOC and incubated at 37°C for 40

minutes in the dark. Controls were used by adding warm PBS equal to the final volume of DiOC/PI treatment to all the samples and standardised on a flow cytometry machine prior to the experimental run. They were then read using FACSCalibur (BD, UK), Filter2. The experiment was carried out in triplicate. Analysis of the data was carried out using Cyflogic and data was compared to untreated cells.

2.7.2. 3-(4,5-dimethylthiazol-2-yl)-2,5-diphenyl-tetrazolium bromide (MTT) assay

Cell viability was determined using a colorimetric 3-(4,5-dimethylthiazol-2-yl)-2,5-diphenyl-tetrazolium bromide (MTT) assay (Sigma, UK). This assay is based on the conversion of MTT to MTT-formazan by mitochondrial enzymes, which is interpreted as reflecting a measure of cell viability. Cells were seeded in a 96-well plate at a density of 1.5-3 $x10^5$ cells /mL for 24 hours to allow adhesion. They were then treated with the various treatment conditions as described above. The MTT assay was performed according to the manufacturers' protocol. After 3.25 hours absorbance was determined at 570 nm and normalised with 690 nm background with a microplate reader (Spectramax 340PC). The optical density was measured as a percentage of untreated cells and repeated between 3-5 times per cell type for experimental replicates with 5 technical replicates per plate.

2.7.3. Lactate dehydrogenase concentration assay

To analyse lactate dehydrogenase concentration in the cell media, a lactate dehydrogenase colorimetric assay (abcam, UK) was carried out. Measuring lactate dehydrogenase allows the evaluation of damage and toxicity to the cell. Lactate

dehydrogenase oxidises lactate to pyruvate producing NADH which reduces the water soluble tetrazolium to the coloured formazon product. This colour can then be measured on a microplate reader. For this assay cells were seeded 3 x10^5 cells/well for 24 hours so they could adhere and consequently treated with the above treatment parameters in phenol red free media. Upon completion the media was collected from the well and assayed according to the manufacturer's instructions. A standard curve was freshly prepared for each plate with the provided standard and assay buffer mix. A reaction mix was freshly prepared with provided assay buffer, substrate mix and enzyme mix. This was added to the collected media in a fresh 96 well plate. The plate was incubated for 30 minutes at room temperature before being read on a microplate reader (Spectramax 340PC) at 450 nm. The background was corrected with the lactate dehydrogenase control standard. A standard curve was plotted of lactic acid nmol vs 450 nm. Lactate dehydrogenase concentrations were applied to this curve and calculated as per the calculation below supplied by abcam (Figure 2.3.) and consequently compared to the untreated cells. All experiments were carried out 3-5 times with 5 technical replicates per plate.

Concentration = La/Sv (nmol/ µl or nM)

La: the amount of lactic acid (nmol) of the sample from the standard curve.

Sv: is the sample volume (µl)

Figure 2.3. Lactate Concentration Equation
Using this equation the concentration of lactate for each sample was calculated using the recorded amount given as a nmol readout from the microplate reader.

2.7.4. Bromodeoxyuridine (BrdU) cell proliferation assay

Cells were tested with a bromodeoxyuridine (BrdU) assay to evaluate the cell proliferation rate. This assay measures BrdU incorporation into newly synthesized DNA strands of actively proliferating cells. Partial denaturation of the double strands of the DNA chains allows BrdU detection and assessment of the cells that are synthesizing DNA. The BrdU cell proliferation assay kit from Millipore, UK was used for this evaluation. A blank control was included whereby no cells are placed in a well but the protocol is carried out to ensure that the reagents are reading the cells correctly. A background control was also included whereby cells were present in the well but no BrdU reagent is added. Again, this is a control to ensure that a background control is included for calculations. The cells were incubated in a 96 well plate at a seeding density of 2.5 x 10^5 cells/mL and were allowed to adhere for 24 hours. They were then treated with the above appropriate protocols and 4 hours prior to the incubation completing the cells were incubated with freshly prepared BrdU. Following 4 hours of incubation the cells were fixed with a supplied fixing solution and incubated for 30 minutes at room temperature. Upon completion the cells were washed 3 times with fresh prepared wash buffer that was supplied, blotting dry after the final wash. The detector antibody anti-BrdU was then added as a prediluted solution and incubated for 1 hour at room temperature. The wells were washed as previously described. Goat anti-mouse IgG conjugate was diluted (1:2000) with the conjugate dilute provided and filtered with a 0.22 µm syringe filter prior to use. This was added to the wells after washing and incubated for 30 minutes at room temperature. The wells were washed again as previously described with an additional final wash with distilled water flooding the wells. The plate was patted dry with absorbent paper towels. TMB peroxide substrate was incubated in the wells for 30 minutes at room temperature in the dark. The experiment was stopped with the supplied stop solution added immediately to each well and read using a

spectrophotometer microplate reader (Spectramax 340PC) at dual wavelength of 450/550 nm. Background was subtracted from the final reading and calculations were compared to the untreated readings. Each plate had a 5 technical replicates for each treatment and the plates were repeated 3-5 times.

2.8. AMPK activity analysis

AMPK activity was analysed using the previously described method (Davies *et al.* 1989, Woods *et al.* 1996, Neumann *et al.* 2003). Cells were harvested after their respective treatments with 50 mM HEPES pH 7.4, 50mM sodium fluoride (NaF) , 5 mM sodium pyrophosphate (NaPP), 1 mM ethylenediaminetetraacetic acid (EDTA), 10% glycerol, 1 mM benzamidin, 0.1 mM Phenylmethly sulphonyl fluoride (PMSF), 1 mM dithiothreitol (DTT) buffer containing 1% Triton X-100 through rapid lysis on ice. A slow lysis AMPK positive control was also prepared. AMPK was immunoprecipitated from 50–100 µg of cell lysate using a rabbit anti-pan-β-antibody and protein A-Sepharose (Woods et al 1996). AMPK activity was determined by phosphorylating the synthetic substrate peptide HMRSAMSGLHLVKRR (SAMS peptide) (Davies S.P. et al, 1989) in the presence of 5 mM $MgCl_2$, 0.2 mM [γ-^{32}P] ATP (specific radioactivity ~200 cpm/pmol), and 0.2 mM Adenosine monophosphate (AMP). Activity levels were compared to and measured as a percentage of change untreated cells upon calculation.

2.9. ROS measurement

Cellular ROS was measured using a 2',7'–dichlorofluorescein diacetate (DCFDA) Assay (abcam, UK). DCFDA is a fluorescent dye that allows the measurement of ROS activity through the deacetylation of DCFDA to a non-fluorescent compound. This is then

oxidised by ROS into 2', 7'–dichlorofluorescin (DCF) which is highly fluorescent. Cells were prepared by seeding at 2 x 10^5 cells/well for 24 hours to allow adhesion to the 96-well black bottom plate. The DCFDA incubation was carried out according to the protocol. The cells were stained with 25 μM DCFDA with 1X Buffer that was supplied for 45 minutes at 37°C. The cells were then washed with PBS and treated using the various treatment conditions previously described with phenol red free media in the same conditions as above. The amount of ROS was detected on a fluorescent plate read (FLUOstar Omega, BMG Labtech, UK) with an excitation of 495 nm and emission of 529 nm. The optical density was background subtracted and measured as a percentage of untreated cells after being normalised to cell count. This was carried out 3-5 times for experimental replication with technical replicates of 5 wells per plate per treatment.

2.10. Ca^{2+} activity measurement

Ca^{2+} activity was measured using a Fluo-4 Direct™ Calcium Assay (Invitrogen, UK). Reagents were prepared according to manufacturer's protocol prior to each assay. Cells were prepared by seeding at 3 x 10^5 cells/well for 24 hours to allow adhesion to the 96-well black bottomed plates. They were then treated the various treatment conditions as described above. An equal volume of 2X Fluo-4 Direct™ calcium reagent was added directly to the wells after the treatment and incubated at 37°C for 60 minutes. Fluorescence was measured at excitation 494 nm and emission 516 nm on a fluorescent plate reader (FLUOstar Omega, BMG Labtech, UK). The optical density was measured as a percentage of the untreated cells after being normalised to cell count. This was carried out 3-5 times for experimental replication with technical replicates of 5 wells per plate per treatment.

2.11. Cellular Respiration Analysis

Cellular respiration was measured using a Seahorse Bioanalyser (Seahorse Biosciences, USA). Both mitochondrial respiration (determined by oxygen consumption rate (OCR)) and glycolytic activity (determined by extracellular acidification rate (ECAR)) was measured using this system. MDA-MB231 and MCF10A cells were seeded 2-2.5 $x10^4$ cells/well in specific Seahorse Bioanalyser 24 well plate, 24, 48 or 72 hours prior to the assay depending on treatment. The cells were treated appropriately as previously described with protocol 1, 2, 3 and 4. The sensor cartridge was hydrated with Seahorse sensor media at least 18 hours prior to the assay.

For the mitochondrial respiration experiment, cells were washed twice with freshly prepared unbuffered Seahorse Assay medium that had been supplemented with appropriate glucose and 1% sodium pyruvate, pH 7.4 at 37°C and incubated with this same media an hour prior to the experiment beginning as directed. Oligomycin (1 μG), Carbonyl cyanide-4-(trifluoromethoxy) phenylhydrazone (FCCP) (0.4 μM: MCF10A, 0.2 μM: MDA-MB231) and Antimycin/Rotenone (0.25 μM) were added to the sensor plate in the appropriate dilutions directly prior to the commencement of the calibration and assay (Figure 2.4.A.).

For the glycolytic examination cell were washed twice with freshly prepared unbuffered Seahorse Assay medium supplemented with 1% sodium pyruvate, pH 7.4 at 37°C and consequently incubated with the same media 2 hours prior to the assay beginning. This removes any glucose present in the cells that may disturb the accuracy of the readings. In the sensor plate glucose (4500 g/L), Oligomycin (1 μG), and 2-deoxyglucose (2-DG) (1 Mm) was added (Figure 2.4.B.).

Calculations were normalised to protein level which was harvested and calculated by Bradford assay directly after each experiment. Each experiment was repeated 3-5

times with technical replicates of 4 per plate. Calculations were based on images below taken from Seahorse Biosciences (Figure 2.4.).

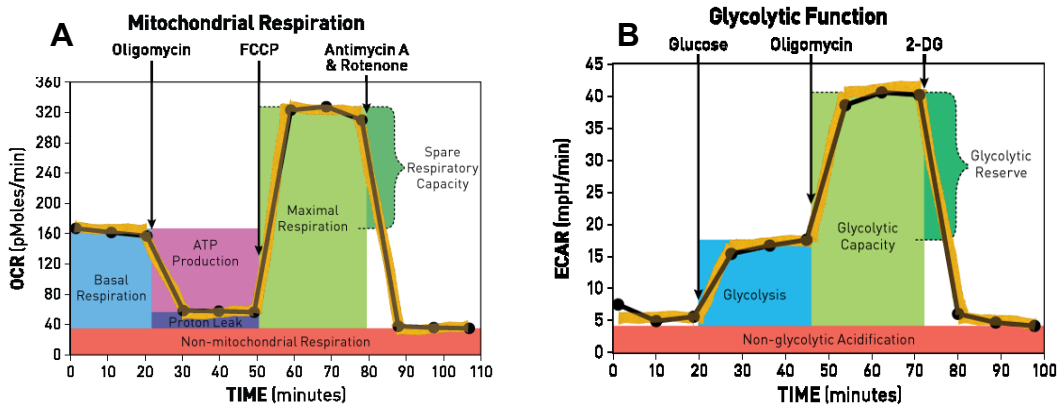

Figure 2.4. Schematic of the Calculations provided through the Seahorse Biosciences Mitochondrial Tests.
(A) Mitochondrial respiration experimental calculation graph. OCR measured in pMoles/min is plotted against time (minutes). Basal respiration is the initial readout with no injection of any reagent. Oligomycin injection allows ATP production to be read as it is an ATP synthase inhibitor and inhibits ATP synthesis in the mitochondria. FCCP is an ETC accelerator and uncoupling agent which increases the potential of hydrogen ions to be passed through the mitochondria's membrane. This gives the potential maximal respiration of the cell type which can also allow spare respiration capacity to be also calculated. This is the measure of the cell's capacity for maximal and basal respiration under stressed conditions. Finally an antimycin and rotenone combination is added that inhibits any mitochondrial respiration giving the non-mitochondrial respiration read out. Proton leak can also be calculated from the antimycin/rotenone injection. **(B)** Glycolytic respiration experimental calculation graph schematic. ECAR is measured as mpH/min and plotted against time (minutes). ECAR is measured and calculate varying different non-mitochondrial respiration parameters after glucose starving. Glucose is reintroduced to the cells after an initial basal reading which once normalised to 2-DG data can give the glycolysis production of the cells. Oligomycin is injected after this which can evaluate the glycolytic capacity of the cell once normalised again to 2-DG data. It also can allow calculation of the glycolytic reserve of the cell. 2-DG inhibits any further glycolysis as the 2-hydroxyl group of glucose is replaced by a hydrogen ion. This allows us to calculate the non-glycolytic acidification of the cell and normalise the data from the other injection reagents.

2.12. Gene expression analysis

For gene expression quantification, quantitative real time-polymerase chain reaction (qRT-PCR) was carried out. Firstly, messenger ribonucleic acid ((RNA)(mRNA)) was isolated from the treated cells using the Qiagen RNeasy kit (Qiagen, UK). The kit was followed as instructed and the samples were quantitated to 0.5 µg/µL using a nanodrop

to normalise RNA amount. Complementary deoxyribonucleic acid (cDNA) synthesis was carried out according to the Thermoscript™ RT-PCR Systems protocol (Invitrogen, UK) using the oligo$(dT)_{20}$ primer method with an incubation of 60 minutes. qPCR was carried out in accordance to TaqMan® Universal Master Mix II, no UNG for primers in Table 2.2 and Platinum® SYBR® Green qPCR superMix-UDG protocol for genes in table 2.3. The 96 well plate was placed in a preheated Applied Biosystems 7500 Fast Real-Time PCR System instrument and run at a cycling program of 50°C for 2 minutes, 95°C for 2 minutes, 45 cycles of 95°C for 15 seconds followed by 56°C for 30 seconds, then a dissociation confirmation step (genes in table 2.3). Any samples that read > 0.2 cycle threshold (Ct) were removed for quality control purposes. Data was calculated using the ΔΔCT method as described in Bookout *et al*., 2006. Samples were normalised to the constitutively expressed α-Tubulin or β-actin (Table 2.2 and 2.3.).

Table 2.2. List of Taqman Probes used for Gene Expression Analysis.

Gene Symbol	Gene Name	Ref Seq mRNA	Taqman Assay ID
IL6	interleukin 6	NM_000600.3	Hs00985639_m1
NFE2L2	nuclear factor, erythroid 2-like 2	NM_001145412.2	Hs00232352_m1
MTOR	mechanistic target of rapamycin	NM_004958.3	Hs00234508_m1
FOXO1	forkhead box O1	NM_002015.3	Hs01054576_m1
AKT1	v-akt murine thymoma viral oncogene homolog 1	NM_001014431.1	Hs00178289_m1
TP53	tumor protein p53	NM_000546.5	Hs01034249_m1
NFKB	nuclear factor of kappa light polypeptide gene enhancer in B-cells 1	NM_001165412.1	Hs00765730_m1
MAPK6	mitogen-activated protein kinase 6	NM_002748.3	Hs00833126_g1
TNF	tumor necrosis factor	NM_000594.3	Hs01113624_g1
FOXO3	forkhead box O3	NM_001455.3	Hs00818121_m1
B-actin	actin, beta	NM_001101.3	Hs01060665_g1

Examined according to TaqMan® Universal Master Mix II, no UNG. Manufactured and supplied by Life Technologies, UK.

Table 2.3. List of Primer Sequences used for Gene Expression Assays.

Primer	Primer Sequence
HDAC1 Forward	5' AGAATGCTGCCGCACGCACC 3'
HDAC1 Reverse	5' CGAGATGCGCTTGTCAGGGTCG 3'
HDAC6 Forward	5' GATGGGCCTTGCCAGTGGCC 3'
HDAC6 Reverse	5' AGCAGGGGTGGTGGGTCTCC 3'
SirT1 Forward	5' GACTGGACTCCAAGGCCACGG 3'
SirT1 Reverse	5' CAGGTGGAGGTATTGTTNCCGGC 3'
Tubulin Forward	5' GCCAAGCGTGCCTTTGTTC 3'
Tubulin Reverse	5' CACACCAACCTCCTCATAATCC 3'

Examined according to Platinum® SYBR® Green qPCR superMix-UDG. Manufactured and supplied by Invitrogen, UK.

2.13. Protein expression levels

Following treatment cells were washed with ice-cold PBS twice and homogenised in ice-cold lysis RIPA buffer (Sigma, UK) which was supplemented with 0.1% protease and phosphatase inhibitors (ThermoScientific, UK). Protein extracts were quantified using the Bradford method (Bio-Rad, UK) with a protein standard of bovine serum albumin (BSA). The samples were calculated to 20 µg per lane with NuPage 4x sample buffer (Invitrogen, UK) and water and were denatured at 95°C for 5 minutes. The samples were separated on CriterionXT Bis-Tris pre-casted 4-12% gels at 140 V for 90 minutes. The proteins were transferred from this gel onto a PVDF membrane at 100 V for 60 - 90 minutes in cold 10% Transfer buffer (Bio-Rad, UK) supplemented with 5 % methanol. The membrane was blocked with 2.5% skim milk solution for 60 minutes and then incubated with the primary antibody overnight at 4°C on a shaker. Antibodies were diluted with Tris-buffered saline and Tween (TBST) (10% 10X Tris-buffered saline (TBS) (1 M Tris chloride (Tris.CL) pH 7.4, 5 M sodium chloride (NaCl), 0.1% Tween 20) as follows: SirT 1 (1:1000), histone deacetylase (HDAC) 1 (1:1000), HDAC 6 (1:1000), interleukin 6 (IL6) (1:250), p53 (1:1000), Nrf2 (1:1000), Nuclear factor - κB (NfκB) (1:1000), mTOR (5 µg), AKT (1:1000), AKT-pan (1:1000), VDAC1 (1:1000) and β-Actin

(1:1000) (abcam, UK) (Table 2.4.). Primary antibody was detected by incubating with the corresponding secondary anti-mouse or anti-rabbit HRP-conjugated (1:5000) (Bio-Rad, UK) after several TBST washes. The membrane was visualised with LI-COR BioSciences Odyssey 2.0 infrared imaging system (LI-COR, UK) and the expression levels calculated on the Image J software program. The protein levels were normalised to the constitutively expressed β-actin and relative intensity (R.I.) was compared to untreated cells. Each antibody was tested between 3-5 times per sample.

Table 2.4. List of Antibody's used for Protein Expression Analysis.
List of antibody's used for protein western blot along with secondary animal it was raised on. Final dilution quantities used for these experiments.

Name	Product Name	Secondary Antibody	Dilution
SirT1*	Anti-SIRT1	Mouse	1:1000
HDAC1	Anti-HDAC1	Mouse	1:1000
HDAC6	Anti-HDAC6	Rabbit	1:1000
IL-6	Anti-IL6	Rabbit	1:250
p53	Anti-p53	Mouse	1:500
Nrf2	Anti-Nrf2	Rabbit	1:1000
NFkB	Anti-NFkB p65	Rabbit	1:1000
mTOR	Anti-mTOR	Rabbit	1:1000
AKT1	Anti-AKT1 (phosphor T308)	Rabbit	1:1000
AKT-pan	Anti-pan-AKT	Rabbit	1:500
VDAC1	Anti-VDAC1/Porin	Mouse	1:1000
B-actin	Anti-beta Actin	Rabbit	1:1000

All supplied by abcam, UK except for those marked with * which were supplied by Millipore, UK.

2.14. Global DNA methylation

Genomic DNA (gDNA) was harvested after treatment and collected using a Blood and Cell culture DNA Mini Kit (Qiagen, UK) following manufacturer instructions, and resuspended in 30 µL LC/MS grade water. 100 ng–1 µg of DNA was digested to nucleosides using DNA Degradase Plus (Zymo Research, UK), for a minimum of 3 hours at 37°C. Samples were pre-cleaned by acetonitrile precipitation. The nucleosides were separated on an Agilent RRHD Eclipse Plus C18 2.1 × 100 mm 1.8u column by using the high-performance liquid chromatography (HPLC) 1200 system (Agilent, UK) and analyzed using Agilent 6490 triple quadrupole mass spectrometer. To calculate the concentrations of individual nucleosides, standard curves with known amounts of synthetic nucleosides were generated and used to convert the peak-area values to corresponding concentrations. Quality control threshold for quantification is a signal-to-noise (calculated with a peak-to-peak method) above 10 fmol. Samples were normalised to the untreated cells and repeated 3-4 times with technical replicates of 3 per run.

2.15. *In vivo* translational study

2.15.1. Animal conditions and general treatment

All experiments were performed in compliance with the Animals (Scientific Procedure) Act 1986 under the project licence 70/7502 19b3. All mice were acclimatised for 72 hours prior to experimental protocol and housed in individually ventilated cages (IVC) under a 12h: 12h light cycle (lights on at 0700 off at 1900) at 21-23°C with *ad libitum* access to food and water.

2.15.2. Cell preparation for xenograft model

MDA-MB231 cells were maintained as described in 2.4. and 2.5. to ensure homogenous distribution. The cells were prepared 24 hours prior to injection by replacing media with freshly supplemented media to ensure a robust supply. They were harvested directly prior to injection as described in 2.5. and counted using a haemocytometer to ensure a standardised distribution.

2.15.3. Experimental protocol for translational study

Male Athymic Crl:NU(NCr)-Foxn1^{nu} mice (Charles River, UK) aged 6- 8 weeks were caged in IVC under the conditions described in 2.16.1. Mice were grouped, 5 mice per cage prior to injection and were weighed to ensure no deviation from the mean cohort. Tumourogenicity was achieved by preparing cells as described in 2.16.2. and injecting subcutaneous into the right dorsal flank 5 x10^5 MDA-MB231 cells in 150 µL media per mouse, using a 25 gauge needle. Cages were divided into 5 groups; Control saline, CBD, cisplatin, combination and “priming” treatment. Each group was assigned to 2 cages for a total of 10 mice per group. Tumours were allowed to grow to ~3 mm x 3 mm to a volume of 15-30 mm^3 before injection. Treatments were injected intratumour 3 times a week and tumours measured using calipers at the same time (Figure 2.5.). This was carried out until the mice had completed 6 injections of treatment. Tumours were measured and volumes calculated using the equation below (Figure 2.6.) (Oh *et al.* 2013). Upon completion of treatment, the animals were sacrificed, blood was collected by cardiac puncture and tumours were collected. Blood was collected in plastic EDTA treated tubes (BD, UK) with 1% protease and phosphatase inhibitors and 10% fresh serine protease inhibitor 4-(2-aminoethyl)-benzenesulfonyl fluoride (AEBSF) to ensure no coagulation and clotting. The EDTA

treated tube was spun for 15 minutes in a cooled centrifuge at 4°C at 12500 RPM. The supernatant was collected into a fresh Eppendorf tube and stored at -80 °C. Tumour size was measured prior to sacrifice and stored at -80 °C.

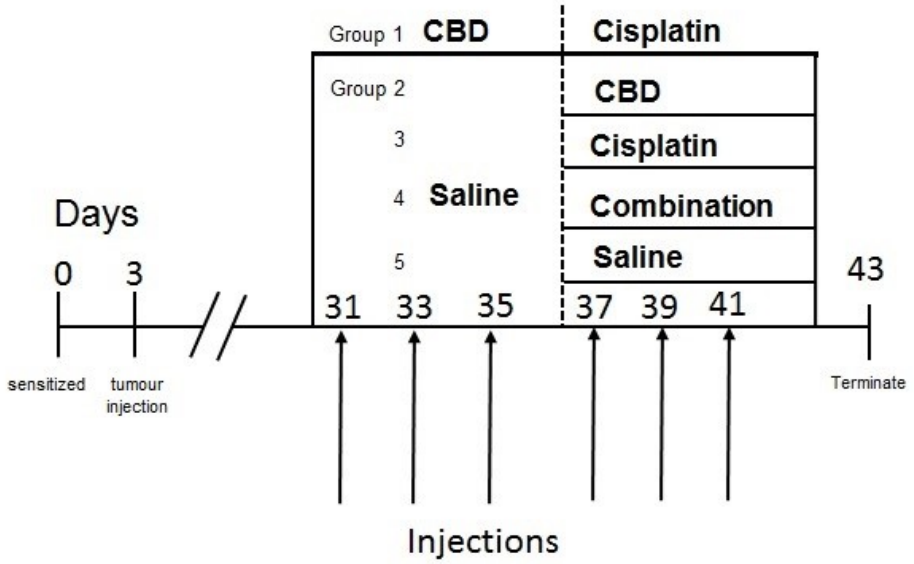

Figure 2.5. Injection Timeline.
Schematic of the experimental protocol and layout of injection protocol beginning with sensitization for 72 hours. After 3 days the MDA-MB231 tumours were injected and allowed to grow. Injections were performed on day 31, 33 and 35 along with calliper measurement. The treatments were changed accordingly for days 37, 39, 41. The animals were terminated on day 43.

$$\frac{(L \times W^2)}{2}$$

Figure 2.6 Tumour Volume Equation.
Tumours were measured using a callipers to determine the length (L) and width (W). Using these measurements volume could be calculated. This ensured that the both the tumours and animals were monitored for experimental and animal welfare.

2.16. Statistical Analysis

All statistical analysis was carried out using GraphPad Prism (San Diego, US) unless otherwise stated. Data is presented as mean ± standard error (SEM). Normality was confirmed with a D'Agostino-Pearson omnibus test prior to statistical analysis. Statistical significance was calculated using Student's t-test when comparing between two treatments or one-way ANOVA with Tukey post-hoc test for multiple comparisons between the data, dose titration comparison analysis. Significance was accepted at the level of * $p<0.05$, * $p<0.01$, ***$p<0.001$.

Chapter 3

The effect of CBD treatment on Cancer cells

3. The effect of CBD treatment on cancer cells

3.1. Introduction

3.1.1. The use of CBD in cancer treatment

The use of CBD as an anti-tumour agent has been shown in several cancer cell lines due to its anti-inflammatory and anti-proliferative mechanisms (Section 1.3.4.) (Guzmán 2003, McAllister *et al.* 2011, Shrivastava *et al.* 2011, Aviello *et al.* 2012, Velasco *et al.* 2012, Ramer *et al.* 2013, Romano *et al.* 2014). CBD does not bind to the CB_1 receptor and does not have any psychological effects as previously mentioned which make it an ideal candidate in clinical studies (Section 1.3.3.1.) (Guzmán 2003, McAllister *et al.* 2011, Velasco *et al.* 2012). Much preclinical work has been carried out using CBD however there has been no translation to human cancer trial even due to the successful use of synthetic and phytocannabinoids in MS and pain relief (Section 1.3.4.) (Guzmán 2003, Barnes 2006, Blake *et al.* 2006, Borgelt *et al.* 2013). Recent patents have surfaced suggesting a surge in CBD cancer research in human trials in the near future (McAllister and Desprez 2014, Sanchez *et al.* 2014).

3.1.2. Variations to CBD treatment

Previous studies looking at the anti-cancer properties of CBD have used a wide range of incubation protocols, including a variety of cancer cell lines, incubation times and a broad range of concentration ranging from 0.1 μM to 200 μM (Section 1.3.4.) (Ligresti *et al.* 2006, McAllister *et al.* 2011, Shrivastava *et al.* 2011, Aviello *et al.* 2012, De Petrocellis *et al.* 2012, Ramer *et al.* 2012, Ramer *et al.* 2013, Macpherson *et al.* 2014, Romano *et al.* 2014). In order to study the potential “priming” properties of CBD it is important to establish a working protocol that takes into account the potential translatable nature of the research. With this in mind breast cancer cells (MDA-MB231)

and their control counterpart (MCF10A) were selected for the establishment of protocol conditions. Much work has been carried out with phytocannabinoids on MDA-MB231 cells, however, its molecular mechanism of action is not fully characterized (Ligresti *et al.* 2006, Shrivastava *et al.* 2011, Takeda *et al.* 2012). Subsequently, other cancer cell lines including colon (HT29), lung (A549), liver (HepG2) and a mitochondrial altered cell line (Rho0) were used to assess the universality of the initial findings. Based on the literature, two time points were selected for the studies, acute (1 hour) and prolonged (24 hours), while the concentration of CBD was kept at a lower range (0.1 µm-5 µM) in order to mimic *in vivo* levels (Lim *et al.* 2011, Shrivastava *et al.* 2011, De Petrocellis *et al.* 2012).

3.1.3. CBD's role in cellular regulation

Once optimal working conditions with CBD had been established, the route and mode of action was examined to observe what alterations in cellular regulation occurred. CBD has been reported to increase Ca^{2+} and ROS concentrations in cancer cells leading to apoptosis (Section 1.3.4.) (Shrivastava *et al.* 2011, De Petrocellis *et al.* 2012, Valvassori *et al.* 2013). The role of CBD in the mitochondria has not been elucidated yet however, there has been suggesting of its alteration in the functionality of the mitochondria and binding to receptors on the mitochondrial membrane (Athanasiou *et al.* 2007, Bénard *et al.* 2012, Rimmerman *et al.* 2013, Valvassori *et al.* 2013). Furthermore, CBD has been shown to regulator cell death through inhibiting AKT activity (Shrivastava *et al.* 2011). A full understanding of the cell death regulators controlled by CBD has not been identified. The role of CBD in inhibiting cell death through AKT and potentially through the mitochondria were key targets in the study shown here. Key aspects of mitochondria's function and regulation were analysed in both cancer lines and control cells.

3.2. Aims of study

- To examine the optimal working dose and treatment conditions of CBD in both cancer and control cells.
- Elucidate CBD's mode of action in mitochondrial regulation.
- Measure CBD's potential as a "priming" agent.

3.3. Acute treatment (1 hour) with CBD

3.3.1. Cell viability following CBD treatment

3.3.1.1. Cancer cells assessment of cell viability following acute CBD treatment

Cancer cells were exposed to increasing concentration of CBD (0.1 μM, 0.5 μM, 1 μM, 2.5 μM, 5 μM) for 1 hour (acute) (Section 2.6.1.) (Figure 3.1.). Cell viability was initially assessed using a fluorescence-activated cell sorting (FACS) analyser. The cells were collected and incubated with PI to test for viability (Section 2.7.1.). No changes in cell viability levels were observed compared to untreated cells using FACS analysis.

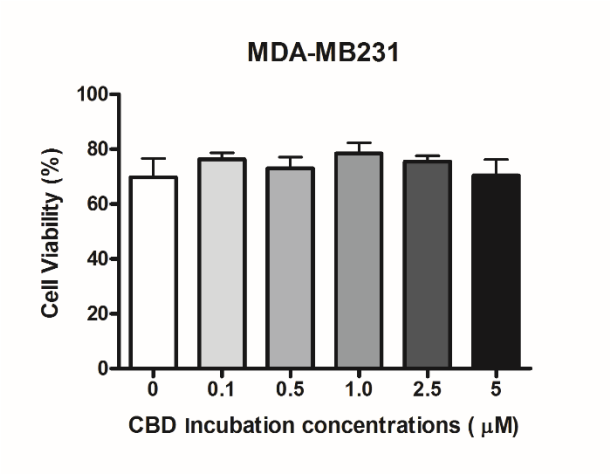

Figure 3.1. 1 hour CBD Cell Viability Analysis on MDA-MB231 cells.
MDA-MB231 cells were treated for 1 hour with CBD and with PI for FACS analysis of cell viability. Data shown is repeated 3 times and is represented as mean ± SEM.

Cell viability can be measured using a lactate dehydrogenase assay which corresponds to cellular damage and toxicity (Section 2.7.3.) (Figure 3.2). Acute (1 hour) CBD treatment showed a trend to increase in lactate dehydrogenase concentration finally reaching significance following 5 μM CBD (127.7 ± 6.35 %) ($p<0.05$) treatment.

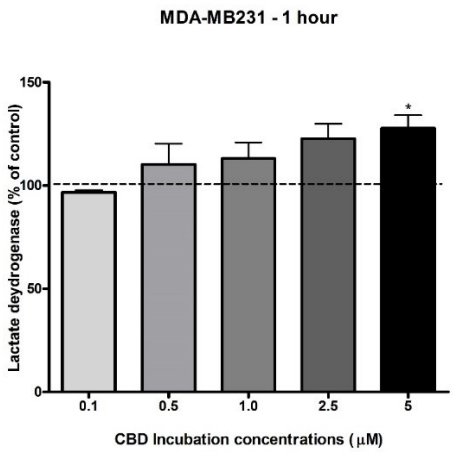

Figure 3.2. The effect of CBD on lactate dehydrogenase concentration in MDA-MB231 cells following 1 hour treatment.
MDA-MB231 cells were treated with CBD 1 hour prior to extraction of the media to analyse for lactate dehydrogenase production. Data shown is repeated 3 times with 5 technical replicates per plate. Data is represented as mean ± SEM. *p<0.05, *vs* Untreated.

3.3.2. CBD's effect on lactate dehydrogenase concentration in control cells following acute treatment

There was no change in cell viability following acute treatment of CBD in control cells (Figure 3.3).

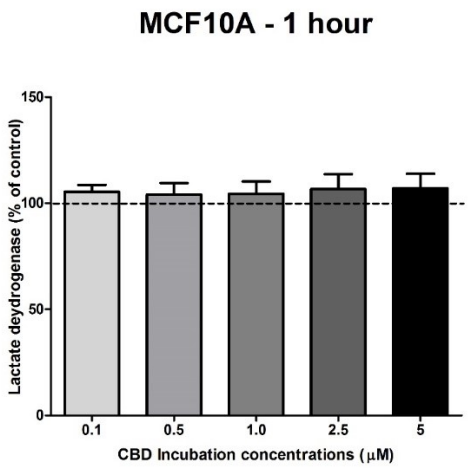

Figure 3.3. The effect of CBD on lactate dehydrogenase concentration following acute treatment in MCF10A cells.
Control cells were treated with CBD for 1 hour prior to extraction of the media to analyse for lactate production. Data shown is repeated 3 times with 5 technical replicates per plate. Data is represented as mean ± SEM.

3.3.3. ROS concentration levels

3.3.3.1. Cancer cells ROS levels were measured following acute treatment of CBD

ROS concentration levels were measured after 1 hour of CBD treatment using a DCFDA assay (Section 2.9.). Cancer cells showed a significant increase in ROS levels from 0.5 μM CBD (1.11 ± 0.047 arbitrary units (A.U.)) ($p<0.05$) ($p<0.001$) (Figure 3.4.). This effect increased with increasing CBD; 1 μM CBD (1.30 ± 0.078 A.U.) ($p<0.01$), 2.5 μM CBD (1.469 ± 0.0821 A.U.) ($p<0.001$) and 5 μM CBD (1.84 ± 0.149 A.U.) ($p<0.001$).

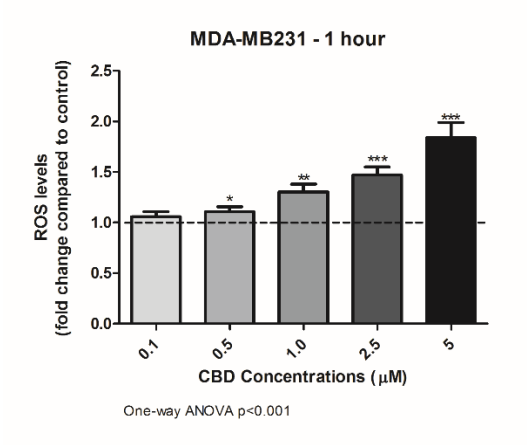

Figure 3.4. MDA-MB231 cell's ROS levels after acute CBD treatment.
MDA-MB231 cells were treated with CBD for 1 hour. ROS levels were measured after incubation. Data shown is repeated 3 times with 5 replicates per plate and is normalised to cell count. Dashed line represents untreated levels. Data is represented as mean ± SEM. *$p<0.05$, **$p<0.01$, ***$p<0.001$ *vs* Untreated.

3.3.3.2. Control cells ROS levels measured following acute CBD treatment

ROS concentration was altered following acute CBD treatment. An initial increase in ROS levels was observed following 0.1 μM CBD treatment (1.08 ± 0.029 A.U.) ($p<0.05$) (Figure 3.5.). However, this effect was reversed with increasing CBD showing a reduction in ROS concentration; 2.5 μM CBD (0.88 ± 0.019 A.U.) ($p<0.001$), 5 μM CBD (0.83 ± 0.019 A.U.) ($p<0.001$).

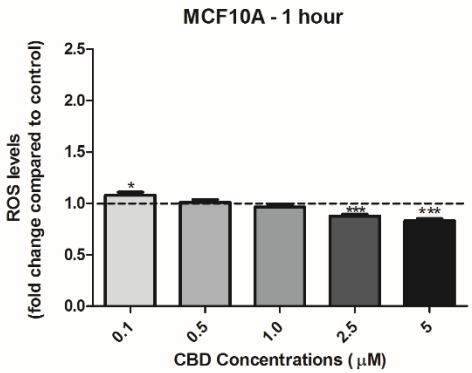

Figure 3.5. MCF10A cell's ROS concentration following acute CBD treatment
Control cell's ROS activity concentrations were measured following acute 1 hour CBD treatment. Data shown is repeated 3 times with 5 replicates per plate and is normalised to cell count. Dashed line represents untreated levels. Data is represented as mean ± SEM. *p<0.05, ***p<0.001 *vs* Untreated.

3.3.4. Mitochondrial function analysis on acute CBD treatment

3.3.4.1. Cancer cells mitochondrial function following acute CBD treatment

Mitochondrial analysis was carried out using a Seahorse Bioanalyser which measures mitochondrial and non-mitochondrial respiration along with several key mitochondrial factors associated with mitochondrial function through oxygen consumption that is linked to their activity (Section 2.11.). Basal mitochondrial OCR was significantly increased following acute CBD treatment, at 0.5 μM CBD (66.88 ± 6.377 pMoles/min) ($p<0.05$), 1 μM CBD (104.1 ± 23.71 pMoles/min) ($p<0.05$), 2.5 μM CBD (119.9 ± 17.57 pMoles/min and 5 μM CBD (129.6 ± 34.36 pMoles/min) ($p<0.05$) (Untreated, 50.44 ± 13.52 pMoles/min) (Figure 3.6.A.). Non-mitochondrial respiration had a trend to decrease reaching significance with 2.5 μM CBD (18.83 ± 2.686 pMoles/min) ($p<0.01$) and 5 μM CBD (18.33 ± 3.667 pMoles/min) ($p<0.05$) (Figure 3.6.B.).

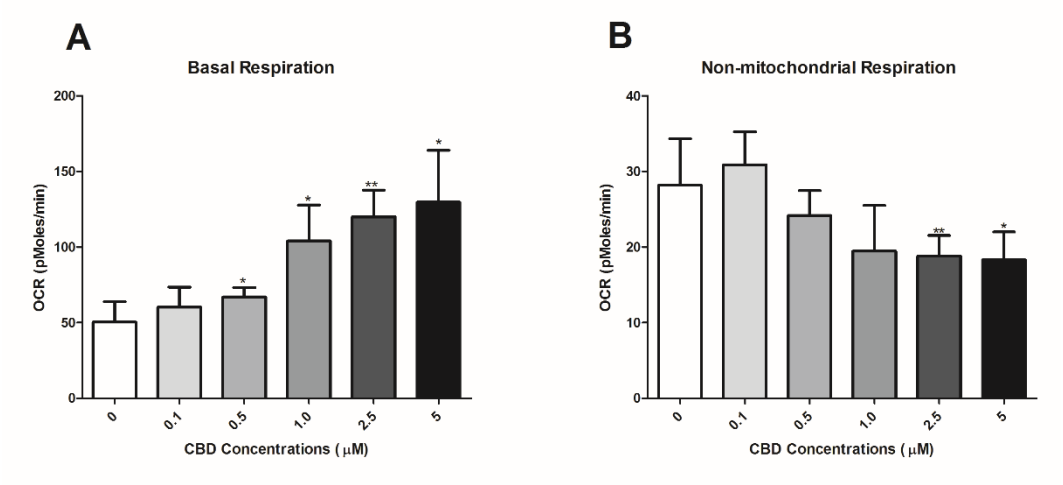

Figure 3.6. Mitochondrial Respiration Analysis following acute CBD treatment on MDA-MB231 cells.
MDA-MB231 cells were treated with CBD for 1 hour prior to mitochondria functional analysis. **(A)** Basal mitochondrial respiration after 1 hour and **(B)** non-mitochondrial respiration were extracted from the experimental data. Data shown is repeated 3 times with 4 technical replicates per plate. Data is represented as mean ± SEM. *p<0.05, **p<0.01 *vs* Untreated.

A dose dependant increase in relative ATP production levels was observed as CBD treatment increased from 0.5 μM CBD (54.83 ± 4.684 pMoles/min) (p<0.01) compared to untreated cells (37.51 ± 8.913 pMoles/min) (Figure 3.7.A). This increase continued as the doses of CBD increased; 1μM CBD (60.49 ± 12.80 pMoles/min) (p<0.05), 2.5 μM CBD (78.01 ± 13.16 pMoles/min) (p<0.01), 5 μM CBD (69.16 ± 16.79 pMoles/min) (p<0.05). A significant dose dependant increase in proton leak was also observed with all concentrations of CBD; 0.1 μM CBD (14.45 ± 1.709 pMoles/min) (p<0.05), 0.5 μM CBD (15.22 ± 1.431 pMoles/min) (p<0.05), 1 μM CBD (21.59 ± 3.216 pMoles/min) (p<0.01), 2.5 μM CBD (26.57 ± 4.430 pMoles/min) (p<0.01) and 5 μM CBD (32.23 ± 9.481 pMoles/min) (p<0.01) (Untreated, 5.839 ± 3.298 pMoles/min) (Figure 3.7.B). A dose dependant increase was also observed with maximal respiration that reached significance with 0.5 μM CBD (81.90 ± 8.026 pMoles/min (p<0.05) and continued as the dose increased to 1 μM CBD (84.87 ± 19.39 pMoles/min) (p=0.1), 2.5 μM CBD (115.1 ± 22.45 pMoles/min) (p<0.05) and 5 μM CBD (124.4 ± 26.35 pMoles/min) (p<0.05) (Untreated, 57.09 ± 13.87 pMoles/min) (Figure 3.7.C).

Interestingly, the spare respiration capacity of the cells showed a biphasic effect. There was a trend to increase with 0.1 μM CBD treatment that was reduced to levels similar to untreated cells as CBD treatment increased to 0.5 μM and 1 μM CBD. This reduction continued as the dose increased with 2.5 μM CBD (-13.56 ± 4.649 pMoles/min) ($p<0.01$) and 5 μM CBD (-25.00 ± 5.991 pMoles/min) ($p<0.01$) (Untreated, 6.650 ± 2.670 pMoles/min) (Figure 3.7.D).

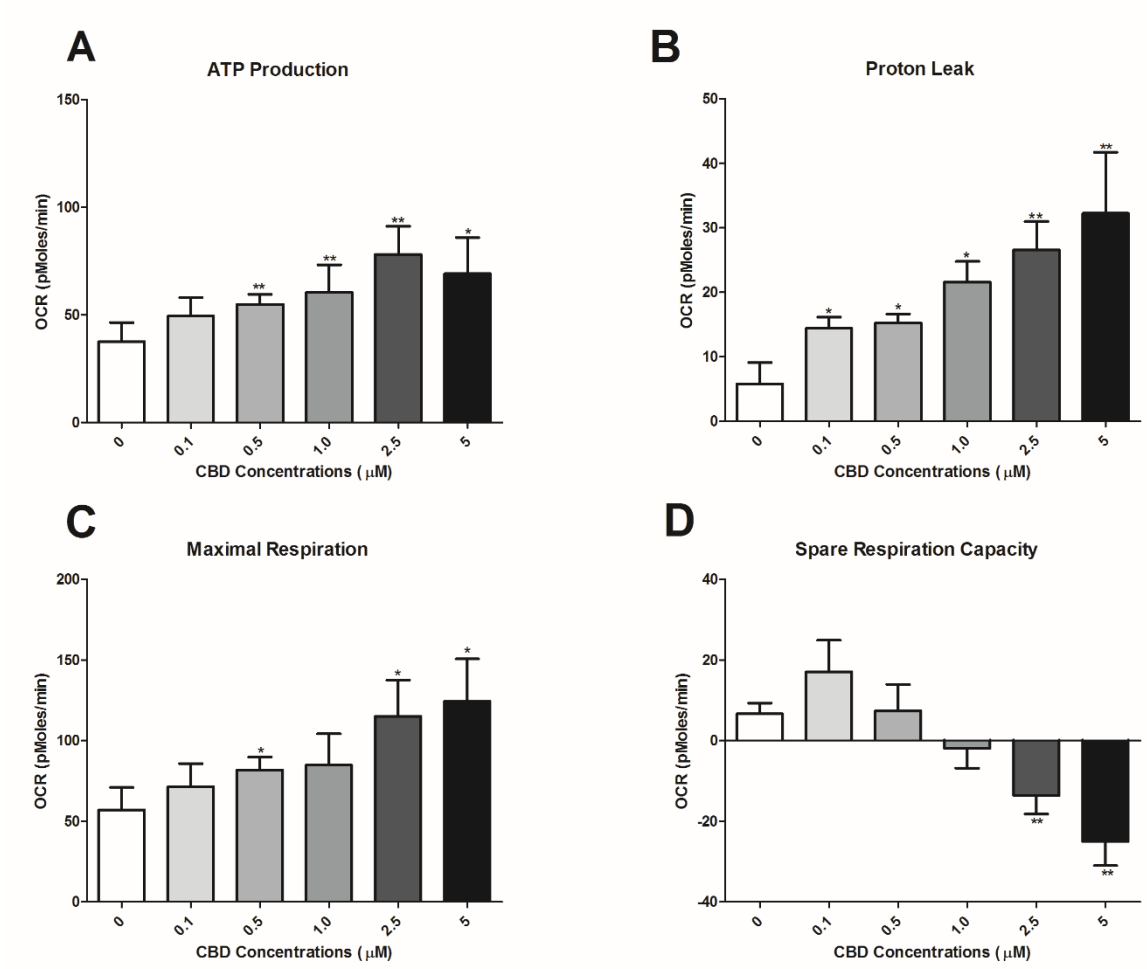

Figure 3.7. Mitochondrial Function Alteration following acute CBD treatment on MDA-MB231 cells.
Assessment of process' associated with the Mitochondria. MDA-MB231 cells were treated with CBD 1 hour prior to examination. **(A)** ATP production was quantified, **(B)** proton leak, **(C)** maximal respiration levels within the mitochondria and **(D)** the spare respiration capacity of the cell were examined. Data shown is repeated 3 times with 4 technical replicates per plate. Data is represented as mean ± SEM. *$p<0.05$, **$p<0.01$, ***$p<0.001$ *vs* Untreated.

3.3.4.2. Control cell's mitochondrial function analysis

After acute treatment with CBD, the control cell's basal mitochondrial respiration increased in a dose dependant manner as CBD treatment increased (Figure 3.8.A.) The increase became significant following 1 μM CBD (162.1 ± 21.95 pMoles/min) ($p<0.05$), 2.5 μM CBD (186.9 ± 32.26 pMoles/min) ($p<0.05$) and 5 μM CBD (196.1 ± 24.15 pMoles/min) ($p<0.01$) (Untreated, 112.7 ± 18.88 pMoles/min). The corresponding non-mitochondrial respiration within the cell was reduced in a dose dependant manner with CBD treatment; 0.5 μM CBD (43.06 ± 4.690 pMoles/min) ($p<0.001$), 1 μM CBD (33.84 ± 7.563 pMoles/min) ($p<0.001$) (Figure 3.8.B.). This reduction levelled as doses of CBD increased to 2.5 μM CBD (35.27 ± 3.719 pMoles/min) ($p<0.001$) and 5 μM CBD (36.60 ± 4.846 pMoles/min) ($p<0.001$) (Untreated, 51.41 ± 14.531 pMoles/min).

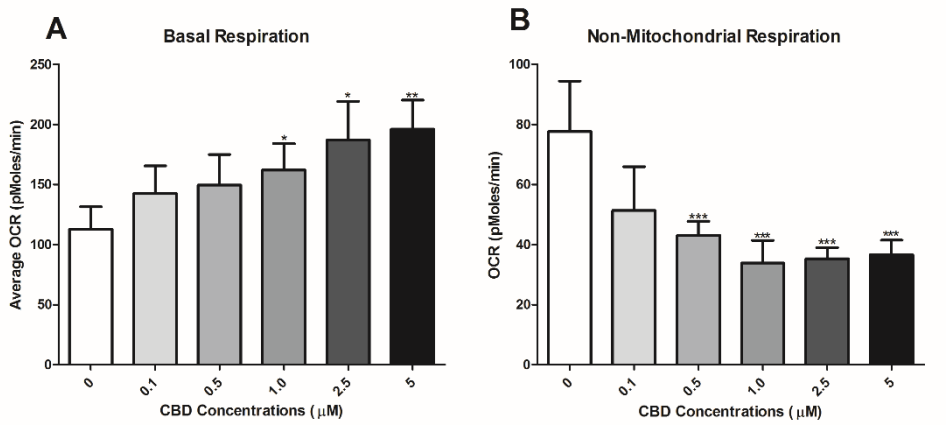

Figure 3.8. Mitochondrial respiration analysis after acute CBD treatment in MCF10A cells. Control cells were treated with CBD for 1 hour prior to mitochondria functional analysis. **(A)** Basal mitochondrial respiration and **(B)** non-mitochondrial respiration were examined. Data shown is repeated 3-5 times with 4 technical replicates per plate. Data is represented as mean ± SEM. *$p<0.05$, **$p<0.01$, ***$p<0.001$ *vs* Untreated.

ATP production levels within the control cells were unchanged with 0.1 μM and 0.5 μM CBD (Figure 3.9.A). However, as the dose of CBD increased, ATP levels reduced in a dose dependent manner; 1 μM CBD (98.69 ± 17.11 pMoles/min) ($p<0.05$), 2.5 μM CBD (86.86 ± 7.868 pMoles/min) ($p<0.001$), 5 μM CBD (48.41 ± 7.614 pMoles/min) ($p<0.001$), Untreated (121.7 ± 26.72 pMoles/min). Proton leak increased in a dose dependant manner as CBD increased; 1 μM CBD (31.71 ± 4.412 pMoles/min) ($p<0.05$), 2.5 μM CBD (42.40 ± 5.481 pMoles/min) ($p<0.01$), 5 μM CBD (41.26 ± 8.803 pMoles/min) ($p<0.05$) (Untreated 20.81 ± 5.275 pMoles/min) (Figure 3.9.B). There was no change in maximal respiration compared to untreated cells (Figure 3.9.C). Treatment with CBD were consistently similar to untreated cells. The cell's spare respiration capacity had a trend to decrease in a dose dependant manner which reached significance at 5 μM CBD (20.42 ± 6.073 pMoles/min) ($p<0.05$) (Untreated, 38.86 ± 10.51 pMoles/min) (Figure 3.9.D).

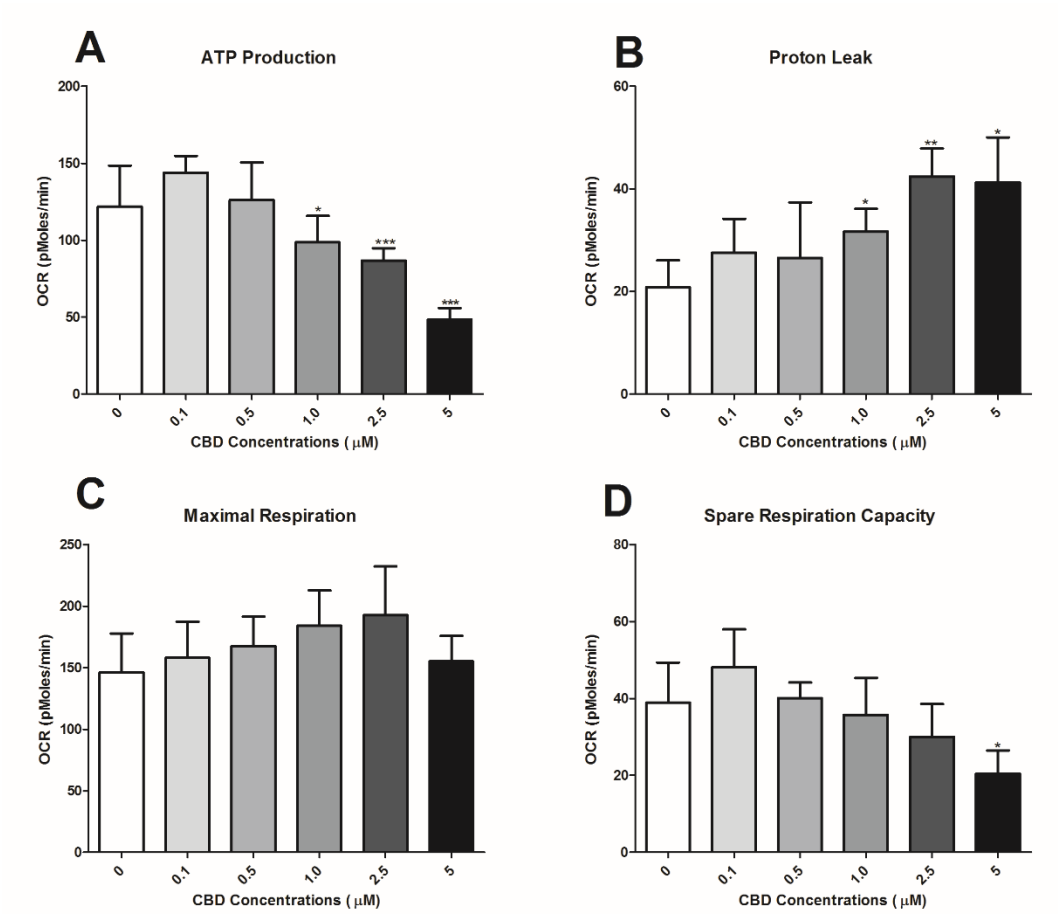

Figure 3.9. Mitochondrial Function Alteration following acute CBD treatment on MCF10A cells.
Assessment of process' associated with the Mitochondria. Control cells were treated with CBD 1 hour prior to examination. **(A)** ATP production levels, **(B)** proton leak, **(C)** maximal respiration levels within the mitochondria and **(D)** the spare respiration capacity of the cell was examined after CBD treatment for 1 hour. Data shown is repeated 3-5 times with 4 technical replicates per plate. Data is represented as mean ± SEM. *p<0.05, **p<0.01, ***p<0.001 *vs* Untreated.

3.3.5. The effects of acute CBD treatment on glycolysis in cancer and control cells

3.3.5.1. Cancer cell's glycolysis analysed following acute CBD treatment

Acute CBD treatment in cancer cells showed a non-significant trend to increase in glycolysis levels (Figure 3.10.A). Furthermore, a slight dose-dependent trend to increase was also observed in glycolytic capacity following CBD treatment that was non-

significant (Figure 3.10.B). There was a similar rate of glycolytic reserve in all treatments of CBD compared to untreated levels (Figure 3.10.C). Non-glycolytic acidification had consistent levels compared to untreated levels as CBD treatment increased (Figure 3.10.D.).

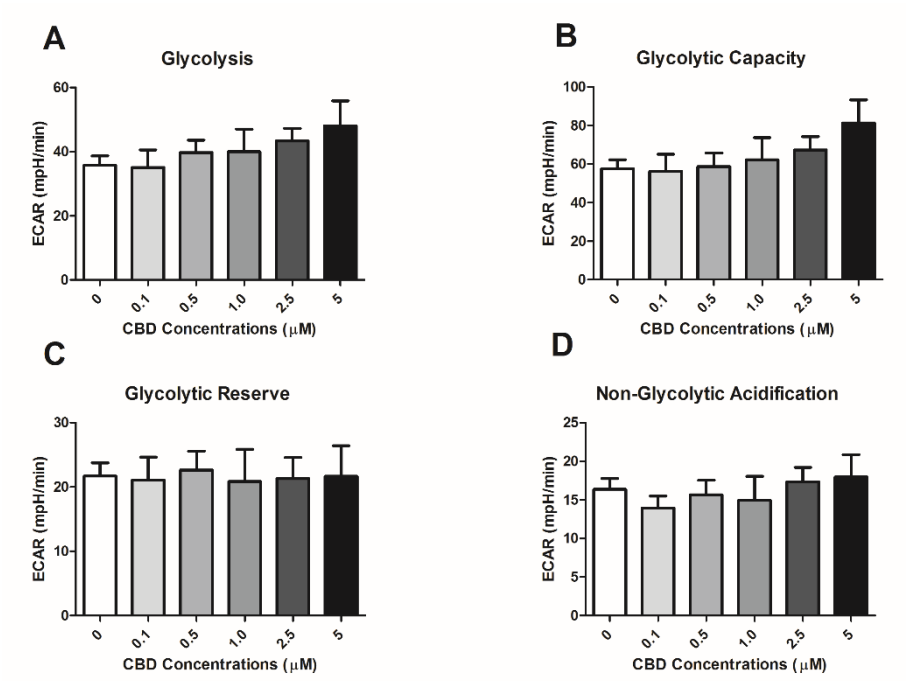

Figure 3.10. The effects of acute treatment of CBD on glycolysis in MDA-MB231 cells
Various parameters of the glycolytic mechanisms were examined after 1 hour of CBD treatment with MDA-MB231 cells. **(A)** Glycolysis was measured along with **(B)** glycolytic capacity. **(C)** Glycolytic reserve and **(D)** non-glycolytic acidification was also examined after 1 hour of CBD treatment. Data shown is repeated 3 times with 4 technical replicates per plate. Data is represented as mean ± SEM.

3.3.5.2. The effect of CBD on control cell's glycolytic activity following acute treatment

When control cells were treated with CBD for 1 hour there was no change in glycolytic events within the cell (Figure 3.11.). Acute treatment with CBD showed no change in glycolysis which remained constant and unchanged compared to untreated levels (Figure 3.11.A). The same effect was observed in glycolytic capacity in that as the dose of CBD increased there was no change compared to untreated levels (Figure 3.11.B). No change in glycolytic reserve was observed as CBD dose increased (Figure

3.11.C). There was no change in non-acidification levels with treatment of CBD (Figure 3.11.D).

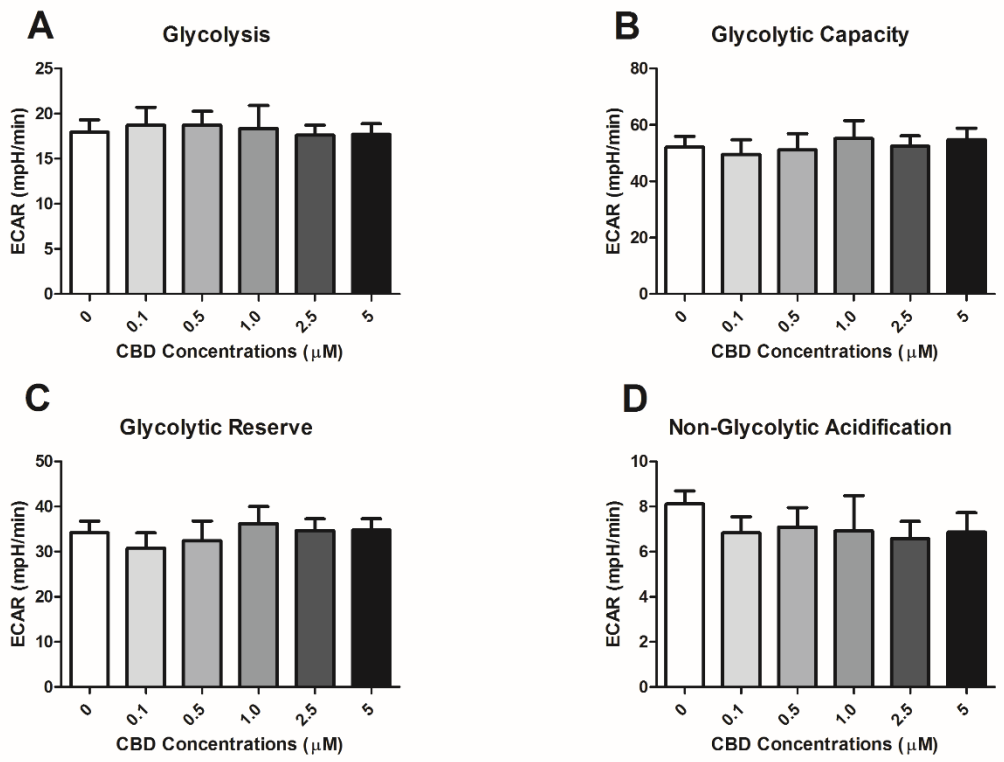

Figure 3.11. Glycolytic Alteration following acute CBD treatment on control cells. Control MCF10A cells were treated with CBD for 1 hour prior to glycolysis analysis. **(A)** Glycolysis, **(B)** glycolytic capacity, **(C)** glycolytic reseve and **(D)** non-glycolytic acidification were examined compared to untreated cells. Data shown is repeated 3 times with 4 technical replicates per plate. Data is represented as mean ± SEM.

3.4. The chronic treatment (24 hours) of CBD in cancer and control cells

3.4.1. CBD's effect on cell viability in cancer and control cells following chronic treatment.

3.4.1.1. The effect of CBD on cancer cell's viability following chronic treatment

Cancer cells were also examined following 24 hours of chronic CBD treatment with the same dose range using FACS (section 2.6.2 and 2.7.1.) (Figure 3.12.). There was no change in cell viability with 0.1 μM CBD, however a significant reduction in viable cancer cells was observed with 0.5 μM CBD (76.01 ± 3.203 %) ($p<0.05$). The reduction in cell viability continued as the dose of CBD increased to 1 μM CBD (65.12 ± 3.239 %) ($p<0.001$), 2.5 μM CBD (47.03 ± 6.538 %) ($p<0.001$) and 5 μM CBD (25.08 ± 3.834 %) ($p<0.001$).

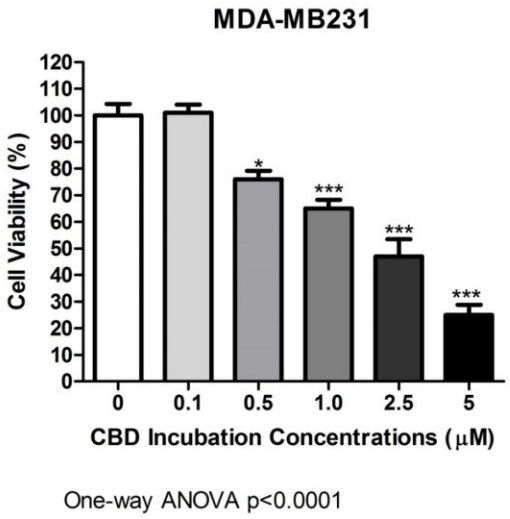

Figure 3.12. Cell Viability following 24 hours of CBD treatment on MDA-MB231 cells. MDA-MB231 cells were treated for 24 hours with CBD and with PI for FACS analysis of cell viability. Data shown is repeated 3 times and is represented as mean ± SEM. *$p<0.05$, ***$p<0.001$ *vs* Untreated.

The reduction in cell viability observed following 24 hours of treatment and FACS analysis was repeated with an MTT viability assay (Section 2.7.2.) (Figure 3.13.). No

changes in cell viability was observed following 0.1 μM CBD treatment, however, a significant reduction in cell viability was detected following 0.5 μM CBD (91.02 ± 2.098 %) ($p<0.05$) treatment. This reduction in viability continued in a dose-dependent manner as CBD treatment increased to 1 μM CBD (87.10 ± 4.531 %) ($p<0.05$), 2.5 μM CBD (78.33 ± 6.243 %) ($p<0.05$) ($p<0.01$) and 5 μM CBD (64.20 ± 6.045 %) ($p<0.01$).

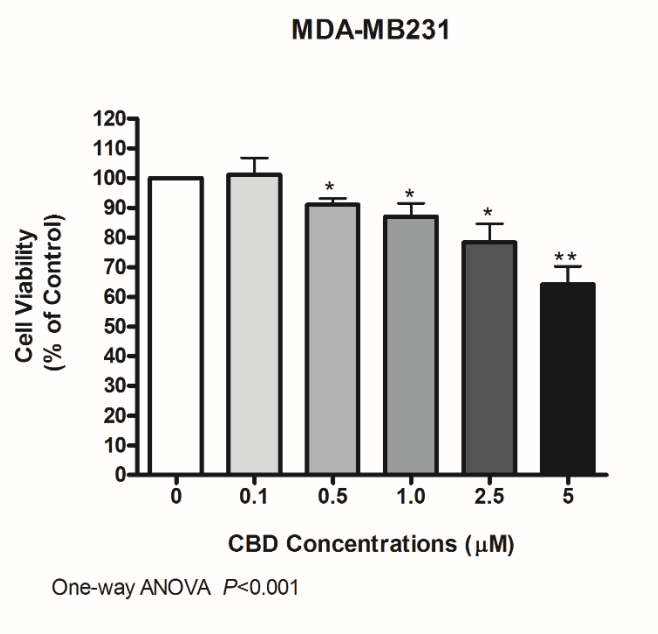

Figure 3.13. The assessment of cell viability following chronic CBD treatment in MDA-MB231 cells with an MTT assay.
Cell viability was determined by MTT assay following chronic CBD treatment. This data shown represents 5 experimental replicates with 5 technical replicates per plate. Data is represented as mean ± SEM. *$p<0.05$, **$p<0.01$ *vs* Untreated.

Cell viability was also assessed with a lactate dehydrogenase assay (Section 2.7.3.) (Figure 3.14.). Following chronic treatment with CBD there was no change in lactate dehydrogenase concentration. The levels of lactate dehydrogenase were similar to untreated cells as the dose of CBD increased.

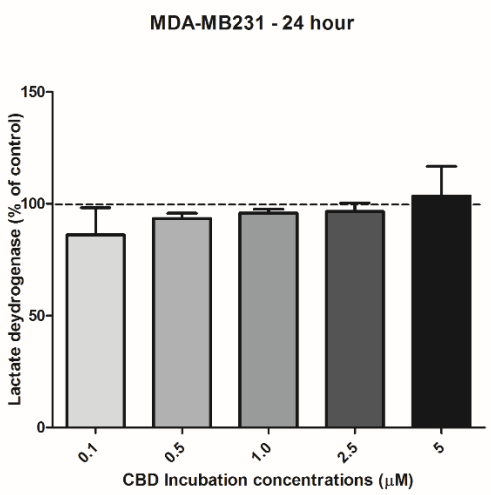

Figure 3.14. Lactate dehydrogenase analysis of MDA-MB231 cells.
MDA-MB231 cells were treated with CBD for 24 hours prior to extraction of the media to analyse for lactate dehydrogenase production. Data shown is repeated 3 times with 5 technical replicates per plate. Data is represented as mean ± SEM.

Following this, cell growth and proliferation were assessed in order to determine if there was an alteration in the actual growth of the cells following CBD treatment using a BrdU cell proliferation assay (Section 2.7.4.). Following chronic CBD treatment in MDA-MB231, no change in cell growth was observed compared to untreated control (Figure 3.15.).

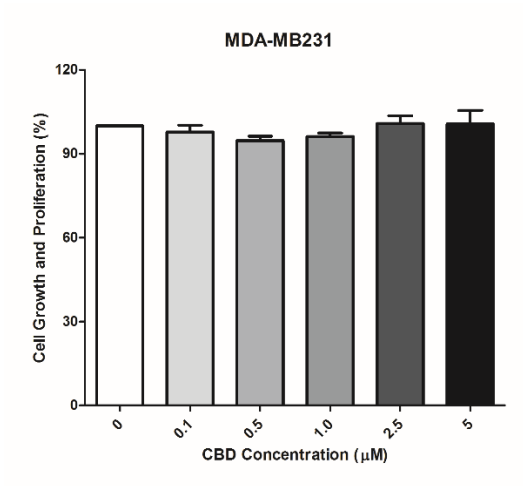

Figure 3.15. The effect of chronic CBD treatment on the cell Growth and Proliferation of MDA-MB231 cells
Cell proliferation was examined following chronic CBD treatment using a BrdU cell proliferation assay. Data shown represents a minimum of 3 experimental replicates with 5 technical replicates per plate. Data is represented as mean ± SEM.

3.4.1.2. The effects of chronic CBD treatment on the cell viability of additional cancer cells

Additional cancer cell lines were treated with CBD under the same conditions for 24 hours to test whether this was a specific effect to MDA-MB231 cells (Figure 3.16.). Colon cancer (HT29) cells showed a reduction in cell viability following 0.5 μM CBD treatment compared to untreated cells (86 ± 3.367 %) ($p<0.05$) (Figure 3.16.A). This reduction continued as the doses of CBD increased; 1 μM CBD (85.75 ± 3.351 %) ($p<0.05$), 2.5 μM CBD (79.5 ± 6.50 %) ($p<0.05$) and 5 μM CBD (72.1 ± 6.36 %) ($p<0.05$), which was similar to MDA-MB231 cells. Liver cancer cells (HepG2) showed a significant reduction of viable cells from 0.1 μM CBD compared to untreated cells (73.80 ± 4.030 %) ($p<0.05$), which again continued to decrease as doses of CBD increased to 0.5 μM (61.80 ± 7.095 %) ($p<0.01$), 1 μM CBD (61.20 ± 3.992 %) ($p<0.001$), 2.5 μM CBD (61.40 ± 4.285 %) ($p<0.001$) and 5 μM CBD (52.80 ± 9.780 %) ($p<0.001$) (Figure 3.16.B). Lung cancer cells (A549) showed no change in cell viability with any CBD treatment (Figure 3.16.C). Breast cancer cells (MCF7) showed a trend to decrease that reached significance following 5 μM CBD (78.25 ± 6.343 %) ($p<0.05$) treatment (Figure 3.16.D.). Cells that had their mitochondrial complex I and IV deleted showed a significant increase in cell viability following 2.5 μM (149.5 ± 15.25 %) ($p<0.05$) and 5 μM CBD (149.3 ± 18.83 %) ($p<0.05$) treatment (Figure 3.16.E).

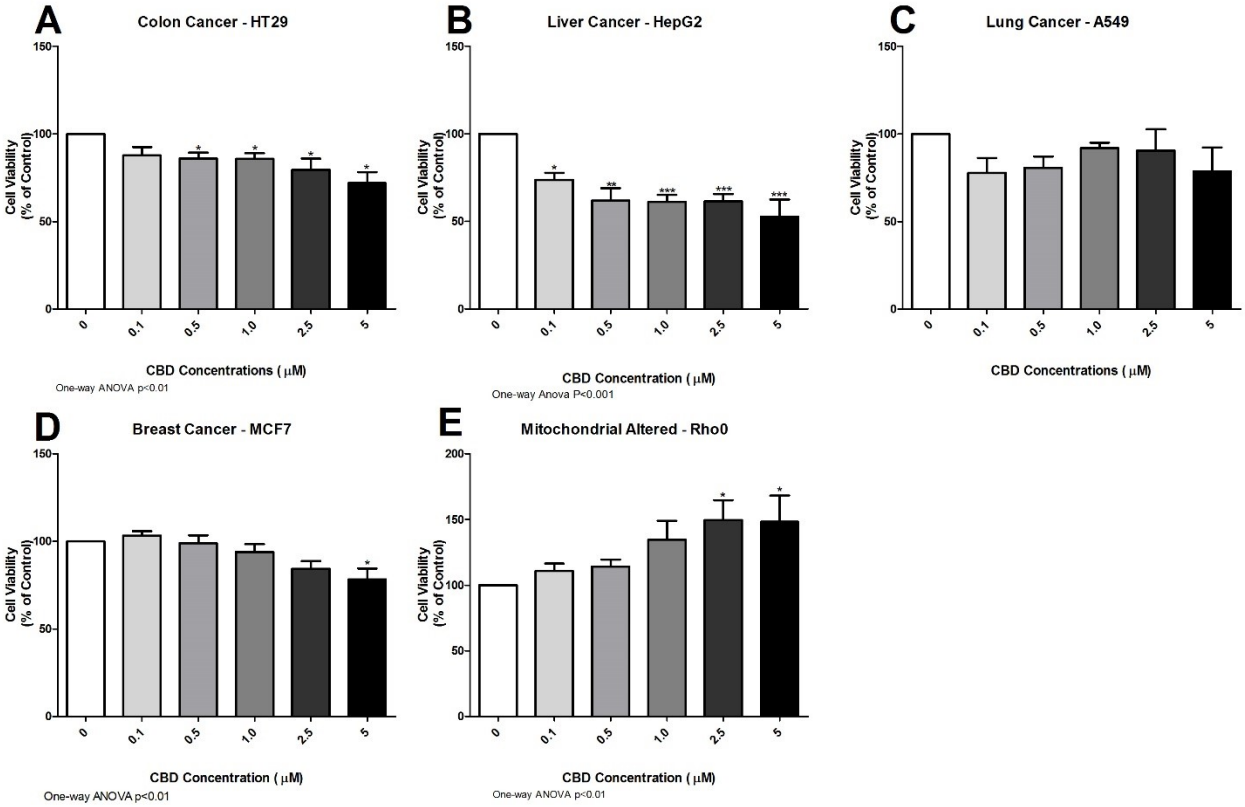

Figure 3.16. The effect of chronic CBD treatment on the viability of other cancer cell lines using an MTT assay.
The effect of CBD on cell viability on different cancer cells was assessed. **(A)** Colon cancer (HT29), **(B)** Liver cancer (HepG2), **(C)** Lung cancer cells (A549), **(D)** Breast cancer (MCF7) and **(E)** cells that had their mitochondrial complexes altered (Rho0). Data shown represents a minimum of three experimental replicates with five technical replicates per plate. Data is represented as mean ± SEM. *p<0.05, **p<0.01, ***p<0.001 *vs* Untreated.

3.4.2. The effect of chronic CBD treatment on control cell's viability

Control cells were tested for any changes to viability following CBD treatment. The cells were treated with CBD for 24 hours and cell viability was analysed using an MTT assay (Section 2.7.2.). There was a trend to decrease in cell viability that became significant following 2.5 μM (82.02 ± 1.732 %) ($p<0.01$) and 5 μM CBD (77.11 ± 3.786 %) ($p<0.05$) treatment (Figure 3.17.).

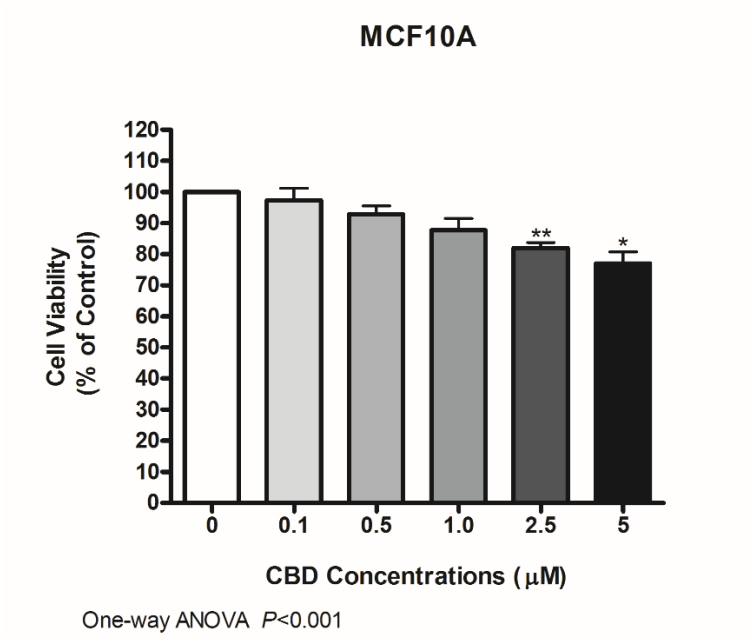

Figure 3.17. The effect of chronic CBD treatment on MCF10A cell viability
Control cells (MCF10A) treated with CBD for 24 hours and analysed using an MTT assay. Data shown is replicated a minimum of 3 experimental replicates with 5 technical replicates per plate. Data is represented as mean ± SEM. *$p<0.05$, **$p<0.01$ *vs* Untreated.

Cell viability was also assessed with the lactate dehydrogenase assay following chronic CBD treatment (Section 2.7.3.) (Figure 3.18.). Chronic CBD treatment showed no change in lactate dehydrogenase concentration compared to untreated levels. There was a trend to decrease in concentration compared to untreated levels though this wasn't significant.

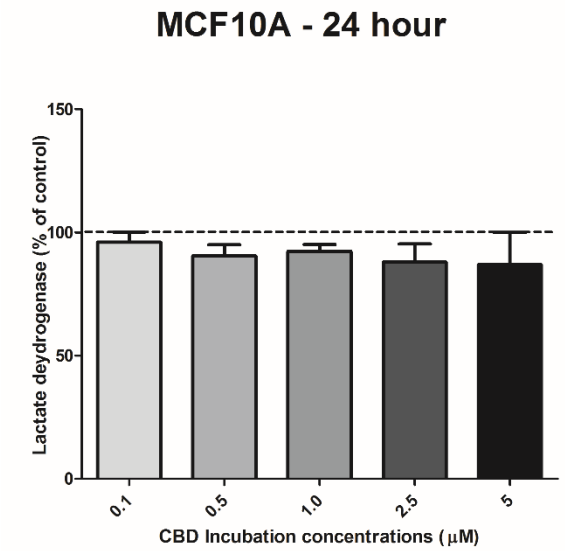

Figure 3.18. The effect of chronic CBD treatment on lactate dehydrogenase concentration in MCF10A cells.
Control cells were treated with CBD for 24 hours prior to extraction of the media to analyse for lactate production. Data shown is repeated 3 times with 5 technical replicates per plate. Data is represented as mean ± SEM.

To assess any alteration to cell growth and differentiation a BrdU assay was carried out following 24 hours of treatment (Section 2.7.4.) There was no change in cell growth and differentiation of the control cells following treatment with CBD for 24 hours (Figure 3.19.). The growth of the cells remained consistent to untreated levels.

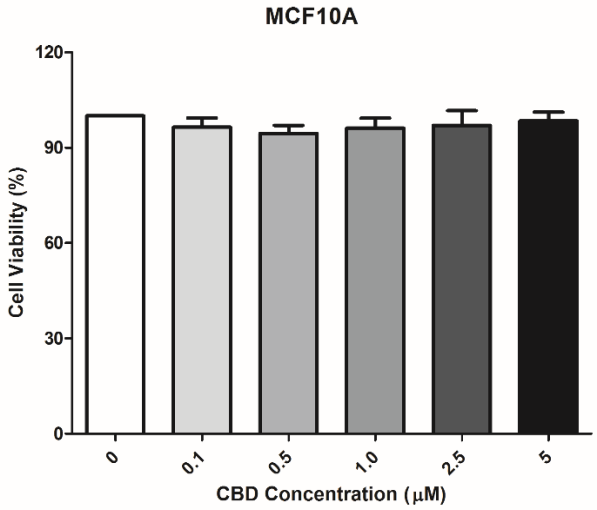

Figure 3.19. MCF10A cell growth and differentiation following treatment with CBD.
The growth and proliferation of normal cells was examined after 24 hours of CBD treatment using a specific BrdU assay. Data shown is repeated a minimum of 3 experimental replicates with 5 technical replicates per plate. Data is represented as mean ± SEM.

3.5. Following chronic CBD treatment, AMPK activity was measured in cancer and control cells.

AMPK activity was measured as AMPK has been shown to be upregulated under stress conditions and increased AMPK can lead to tumourogenesis (Jeon et al., 2012; Hwang et al., 2007). AMPK activity has also been shown to negatively regulate the "Warburg Effect" and be involved in activating the p53 pathway (Section 1.1.3.) (Faubert *et al.* 2013, Faubert *et al.* 2015). Alterations in AMPK activity following CBD treatment could highlight its molecular role in inhibiting tumourogenesis.

3.5.1. Cancer cell's AMPK activity following chronic CBD treatment

Cells were treated with increasing concentrations of CBD for 24 hours before being analysed for AMPK activity alterations (Section 2.8.). A significant decrease in AMPK activity was observed in cancer cells following 0.1 μM CBD treatment (88.60 ± 2.804 %) ($p<0.05$) (Figure 3.20.). The other treatments of CBD did not reach significance however there was a trend to decrease (0.5 μM $p=0.057$, 1.0 μM $p = 0.06$, 2.5 μM $p = 0.06$, 5 μM $p = 0.07$).

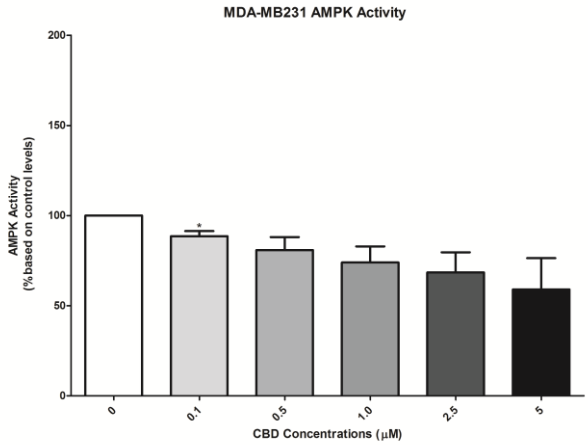

Figure 3.20. The analysis of AMPK activity following chronic CBD treatment in MDA-MB231 cells.
MDA-MB231 cells AMPK activity analysed after 24 hours of CBD treatment. Data shown is a repeated minimum of 4-6 experimental replicates. Data is represented as mean ± SEM. *$p<0.05$ *vs* Untreated.

3.5.2. The analysis of AMPK activity in control cells following chronic CBD treatment

Control cells showed a trend to decrease in AMPK activity that did not reach significance when treated with increasing CBD for 24 hours (Figure 3.21.).

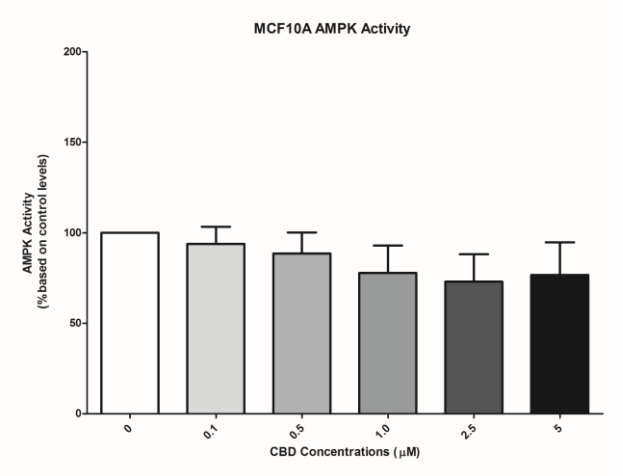

Figure 3.21. The activity of AMPK following chronic CBD treatment in MCF10A cells. MCF10A cells were treated with CBD for 24 hours prior to AMPK activity analysis. Data shown is a repeated minimum of 4-6 experimental replicates. Data is represented as mean ± SEM.

3.6. The effect of chronic CBD treatment on cellular ROS levels

Cell metabolism is tightly controlled through several key mechanisms with one such being ROS (Section 1.1.3.4.) (Brookes *et al.* 2004, Sena and Chandel 2012). ROS can control the cells fate through stimulating cell proliferation at low doses but increasing cell death at high levels (Gupta *et al.* 2012, Sena and Chandel 2012).

3.6.1. Cancer cell's ROS levels following chronic CBD treatment

ROS activity levels were measured following 24 hours of CBD treatment using a DCFDA assay (Section 2.9.) (Figure 3.22). A significant increase was observed following 1 μM CBD (1.09 ± 0.037 A.U.) ($p<0.05$) treatment. This increase continued in a dose dependant manner as the treatment dose increased to 2.5 μM CBD (1.16 ± 0.057 A.U.) ($p<0.05$) and 5 μM CBD (1.289 ± 0.0445 A.U.) ($p<0.001$).

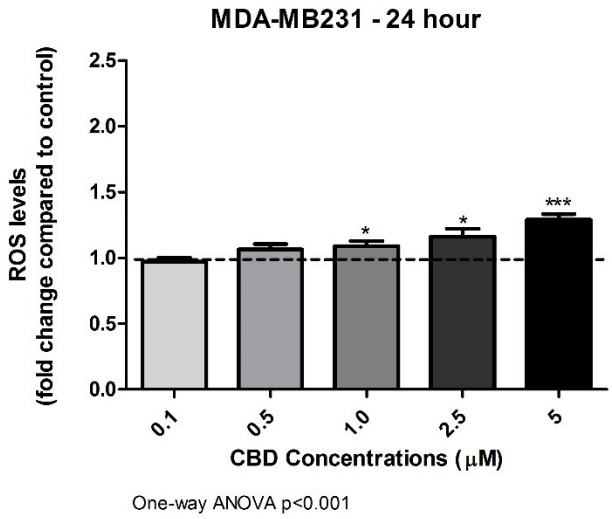

Figure 3.22. The ROS levels in MDA-MB231 cells following chronic CBD treatment. MDA-MB231 cells were treated with CBD for 24 hours. ROS levels were measured after incubation. Data shown is repeated 3 times with 5 replicates per plate and is normalised to cell count. Dashed line represents untreated levels. Data is represented as mean ± SEM. *$p<0.05$, ***$p<0.001$ *vs* Untreated.

3.6.2. The effect of chronic CBD treatment on ROS levels in control cells

No change in ROS levels were observed following a chronic 24 hour treatment with CBD (Figure 3.23).

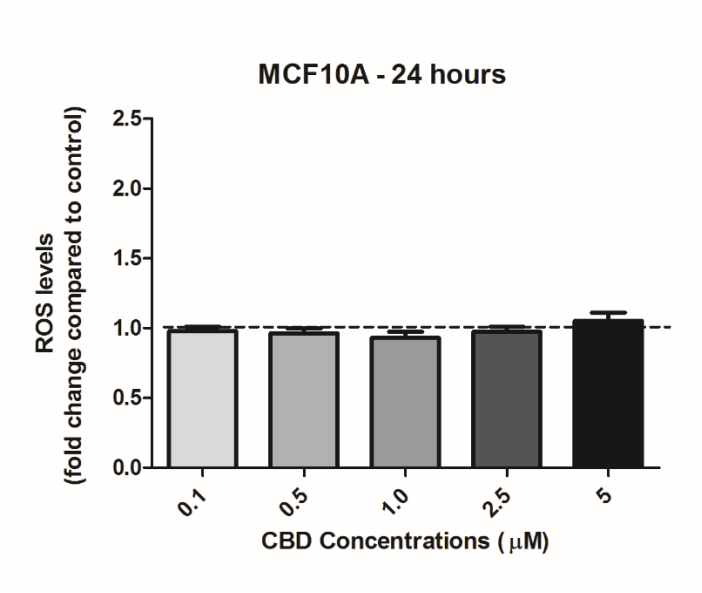

Figure 3.23. The levels of ROS in MCF10A cells following chronic CBD treatment
Control cells ROS activity levels were measured following chronic 24 hours of CBD treatment. Data shown is repeated 3 times with 5 replicates per plate and is normalised to cell count. Dashed line represents untreated levels. Data is represented as mean ± SEM.

3.7. CBD treatment's effect on Ca^{2+} levels following chronic CBD treatment

Ca^{2+} is another important controller of metabolism function and increasing its activity can lead to cell death (Section 1.1.3.3.) (Mathiasen *et al.* 2002, Brookes *et al.* 2004, Prevarskaya *et al.* 2011). The regulation of Ca^{2+} levels within the cell was examined to observe if there was any further loss of control of key regulators of cellular regulation.

3.7.1. Cancer cell's Ca^{2+} levels following chronic CBD treatment

Ca^{2+} concentration levels were measured following 24 hours of CBD treatment by using a Fluo-4 Direct™ Calcium Assay (Section 2.10.). MDA-MB231 cells showed an increase in calcium levels compared to untreated cells; 0.5 μM CBD (1.24 ± 0.049 A.U.) ($p<0.05$), 1μM CBD (1.19 ± 0.049 A.U.) ($p<0.05$), 2.5 μM CBD (1.26 ± 0.033 A.U.) ($p<0.05$), 5 μM CBD (1.895 ± 0.0448 A.U.) ($p<0.05$) (Figure 3.24.). This increase continued as the dose of CBD increased to 5 μM ($p<0.05$).

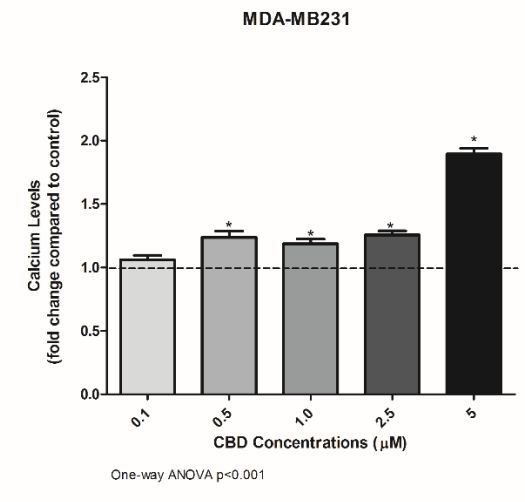

Figure 3.24. Calcium levels were assessed in MDA-MB231 cells following chronic CBD treatment.
Ca^{2+} concentration was measured on MDA-MB231 cells after 24 hours of CBD treatment. Data shown is repeated 3 times with 5 replicates per plate and is normalised to cell count. Dashed line represents untreated levels. Data is represented as mean ± SEM. *$p<0.05$ *vs* Untreated.

3.7.1. The effect of chronic CBD treatment on control cells Ca^{2+} levels

Ca^{2+} levels were increased in control MCF10A cells when treated with CBD for 24 hours (Figure 3.25.). A significant increase was observed from 0.5 μM CBD ($p<0.05$) treatment that continued to increase in a dose dependant manner; 0.5 μM CBD (1.05 ± 0.016 A.U.) ($p<0.05$), 1 μM CBD (1.10 ± 0.021 A.U.) ($p<0.05$), 2.5 μM CBD (1.28 ± 0.021 A.U.) ($p<0.05$), 5 μM CBD (1.40 ± 0.023 A.U.) ($p<0.05$).

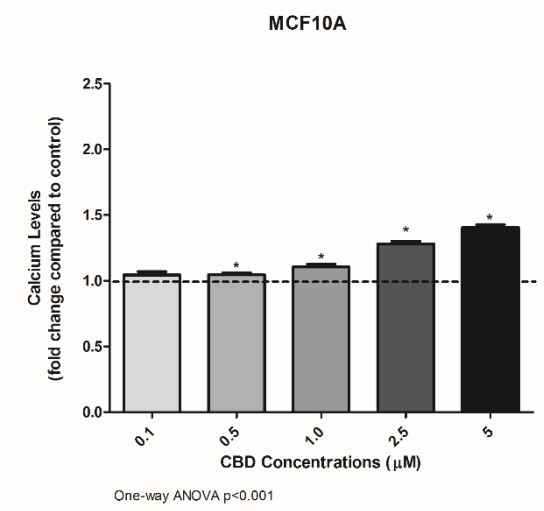

Figure 3.25. MCF10A cell's calcium levels following chronic CBD treatment.
Calcium levels of control cells after 24 hours of CBD treatment. Data shown is repeated 3 times with 5 replicates per plate and is normalised to cell count. Dashed line represents untreated levels. Data is represented as mean ± SEM. *p<0.05 *vs* Untreated.

3.8. Chronic CBD's effect on mitochondrial function

Mitochondrial function is known to be altered in cancer cells compared to control cells (Section 1.1.3.) (Vander Heiden *et al.* 2009, Kroon and Taanman 2014). This alteration is known to affect growth and function of metabolism within cancer cells and CBD is known to interact with the mitochondria (Section 1.1.3.1. and 1.3.4.) (Samudio *et al.* 2009, Vander Heiden *et al.* 2009, Valvassori *et al.* 2013).

3.8.1. The effect of chronic CBD treatment on cancer cell's mitochondrial function

When MDA-MB231 cells were treated with CBD for 24 hours the acute changes previously observed in section 3.2.3.1. on mitochondrial respiration remained and were enhanced following analysis with the Seahorse Bioanalyser (Section 2.11.). Mitochondrial respiration showed a significant increase in OCR compared to untreated following 0.1 μM CBD (61.84 ± 5.521 pMoles/min) ($p<0.05$) treatment (Untreated, 47.50 ± 6.146 pMoles/min) (Figure 3.26.A). This increase in basal mitochondrial respiration continued to increase in a dose dependant manner as CBD increased; 0.5 μM CBD (61.20 ± 5.722 pMoles/min) ($p<0.05$), 1 μM CBD (66.55 ± 8.150 pMoles/min) ($p<0.05$), 2.5 μM CBD (79.69 ± 4.574 pMoles/min) ($p<0.001$), 5 μM CBD (77.98 ± 10.851 pMoles/min) ($p<0.05$). Non-mitochondrial respiration decreased in a dose dependant manner and was significantly lower than untreated cells with 1 μM CBD (66.72 ± 6.458 pMoles/min) ($p<0.05$) and 5 μM CBD (58.67 ± 8.167 pMoles/min) ($p<0.05$) (Untreated, 81.17 ± 15.95 pMoles/min) (Figure 3.26.B).

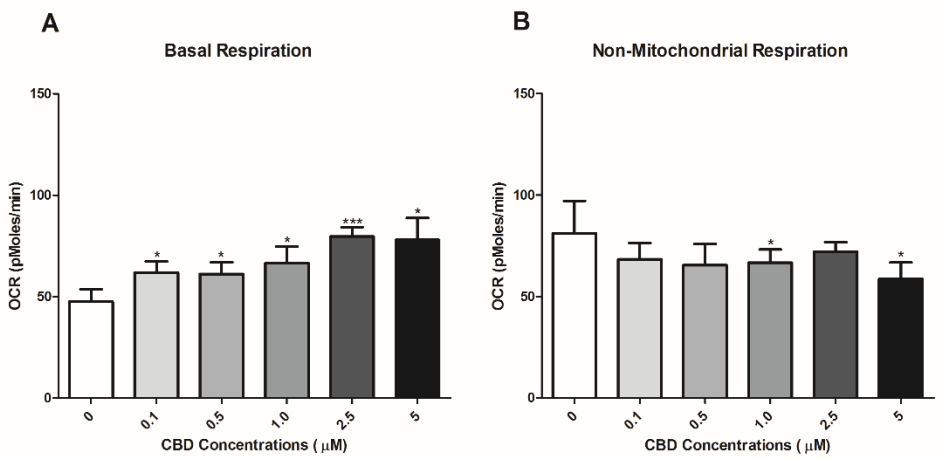

Figure 3.26. Mitochondrial respiration analysis following chronic CBD treatment in MDA-MB231 cells.
MDA-MB231 cells were treated with CBD for 24 hours prior to mitochondria functional analysis. **(A)** Basal mitochondrial respiration and **(B)** non-mitochondrial respiration were extracted from the experimental data. Data shown is repeated 3-5 times with 4 technical replicates per plate. Data is represented as mean ± SEM. *p<0.05, ***p<0.001 *vs* Untreated.

ATP levels were also enhanced in a dose dependant manner as CBD treatment increased; 0.1 μM CBD, 62.83 ± 9.152 pMoles/min, p<0.05; 0.5 μM CBD, 71.87 ± 12.952 pMoles/min, p<0.05; 1 μM CBD, 76.73 ± 14.891 pMoles/min, p<0.05; 2.5 μM CBD, 78.68 ± 11.981 pMoles/min, p<0.01; 5 μM CBD, 84.41 ± 18.771 pMoles/min, p<0.05; Untreated, 39.26 ± 5.164 pMoles/min (Figure 3.27.A.). Proton leak showed no change in activity compared to untreated cells with lower doses of CBD (0.1 μM to 0.5 μM CBD) (Figure 3.27.B.). However, as CBD concentration increased, a dose dependant decrease in proton leak was observed; 2.5 μM (15.02 ± 1.085 pMoles/min) (p<0.05), 5 μM CBD (11.21 ± 2.800 pMoles/min) (p<0.05). Maximal respiration was significantly increased with 0.5 μM CBD (112.5 ± 16.31 pMoles/min) (p<0.05) which continued to increase in capacity in a dose dependant manner; 1 μM CBD (114.1 ± 16.16 pMoles/min) (p<0.05), 2.5 μM CBD (132.3 ± 24.561 pMoles/min) (p<0.05), 5 μM CBD (125.0 ± 23.73 pMoles/min) (p<0.05) (Figure 3.27.C.). No change in spare respiration capacity was observed compared to untreated cells (Figure 3.27.D.). As CBD increased the spare respiration capacity remained consistent with untreated levels.

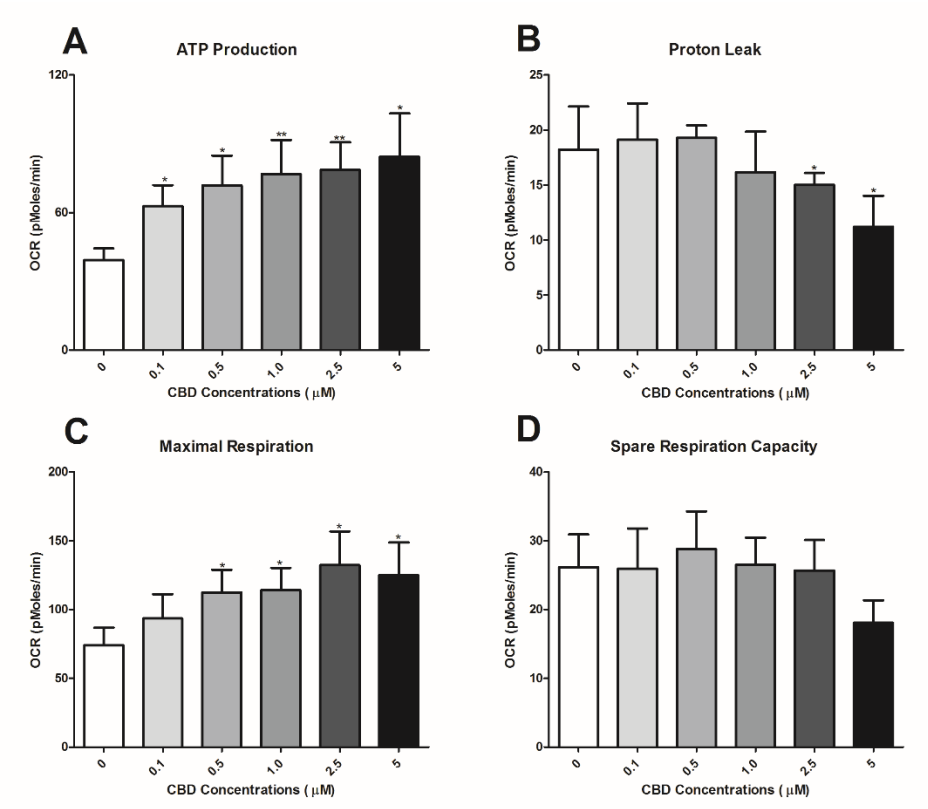

Figure 3.27. The effect of chronic CBD treatment on mitochondrial function in MDA-MB231 cells.
Assessment of process' associated with the Mitochondria. MDA-MB231 cells were treated with CBD 24 hours prior to examination. **(A)** ATP production levels, **(B)** proton leak, **(C)** maximal respiration levels within the mitochondria and **(D)** the spare respiration capacity of the cell were calculated from the extracted data. Data shown is repeated 3-5 times with 4 technical replicates per plate. Data is represented as mean ± SEM. *p<0.05, **p<0.01 *vs* Untreated.

3.8.2. Chronic CBD treatment's effect on mitochondrial function in control cells

The cells basal mitochondrial respiration rates showed no change in OCR compared to untreated cells (Figure 3.28.A.). As CBD increased basal respiration remained similar to untreated levels. Similarly, there was no change in non-mitochondrial respiration of the control cells as CBD treatment doses increased (Figure 3.28.B.).

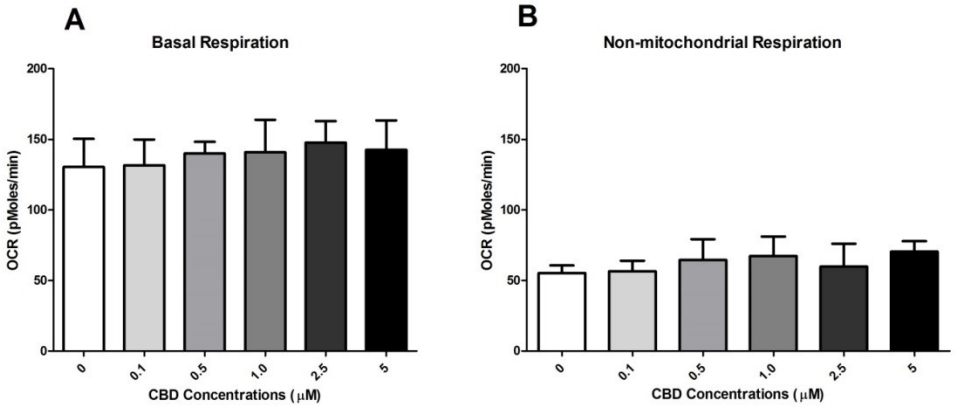

Figure 3.28. Chronic CBD's effect on mitochondrial respiration and non-mitochondrial respiration in MCF10A cells.
Control cells were treated with CBD for 24 hours prior to mitochondria functional analysis. **(A)** Basal mitochondrial respiration and **(B)** non-mitochondrial respiration showed no difference compared to the Untreated cells. Data shown is repeated 3-5 times with 4 technical replicates per plate. Data is represented as mean ± SEM.

No alteration in ATP production levels was observed either compared to untreated levels (Figure 3.28.A). As CBD treatment increased the ATP production levels remained similar to untreated levels. There was a tendency for reduction in proton leak that was significantly reduced with 2.5 μM CBD treatment (13.17 ± 2.717 pMoles/min) ($p<0.05$) and 5 μM CBD (11.97 ± 3.091 pMoles/min) ($p<0.05$) (Untreated, 19.35 ± 1.840 pMoles/min) (Figure 3.28.B.). There was no change in maximal respiration which again remained constant as CBD treatment increased (Figure 3.28.C.) The spare respiration capacity of the cell also remained unchanged compared to untreated cells (Figure 3.28.D.).

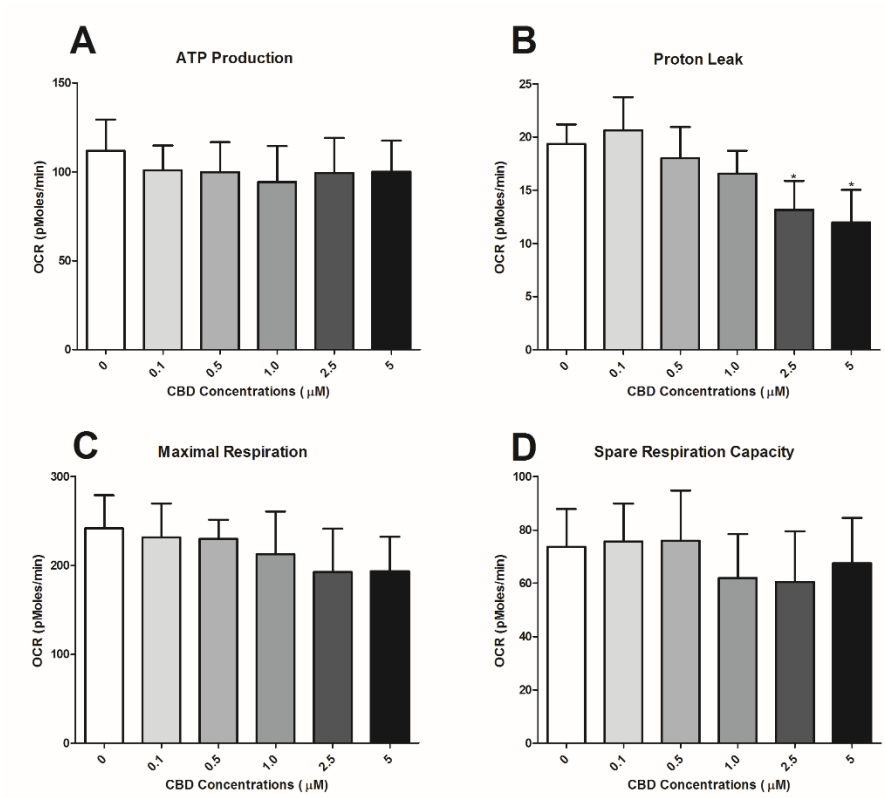

Figure 3.29. Chronic CBD's effect on mitochondrial function in MCF10A cells.
Assessment of process' associated with the Mitochondria. Control cells were treated with CBD 24 hours prior to examination. **(A)** ATP production levels, **(B)** proton leak, **(C)** maximal respiration levels within the mitochondria and **(D)** the cells spare respiration capacity were examined after 24 hours of CBD treatment. Data shown is repeated 3-5 times with 4 technical replicates per plate. Data is represented as mean ± SEM. *p<0.05 *vs* Untreated.

3.9. The effect of chronic CBD treatment on glycolysis

Along with mitochondrial alteration, cancer cells have been shown to upregulate glycolytic activity within the cell (Section 1.1.3.) (Hsu and Sabatini 2008, Vander Heiden *et al.* 2009, Diaz-Ruiz *et al.* 2011). Glycolysis is an anaerobic process that produces less energy than the mitochondria, thus is not as efficient source within the cell (Nelson and Cox 2006, Israelsen and Vander Heiden 2010).

3.9.1. The effect of chronic CBD treatment on cancer cell's glycolysis

Cancer cells showed no change in glycolysis following chronic CBD treatment using the Seahorse Bioanalyser glycotest (Section 2.11.) (Figure 3.30.A.). The levels remained similar to untreated levels as CBD treatment increased. There was also no change in glycolytic capacity which remained similar to untreated cells as CBD increased (Figure 3.30.B.). There was a reduction in glycolytic reserve following 0.1 μM CBD (27.72 ± 5.690 mpH/min) ($p<0.05$) treatment (Figure 3.30.C.). This decrease was constant as the dose of CBD increased; 0.5 μM CBD (28.47 ± 2.479 mpH/min) ($p<0.001$), 1 μM CBD (28.63 ± 4.134 mpH/min) ($p<0.01$), 2.5 μM CBD (25.82 ± 1.554 mpH/min) ($p<0.001$), 5 μM CBD (23.94 ± 4.604 mpH/min) ($p<0.01$) (Untreated, 42.51 ± 7.304 mpH/min). Non-glycolytic acidification was also reduced with 0.1 μM CBD (10.96 ± 0.7425 mpH/min) ($p<0.001$) (Figure 3.30.D.). This decrease also remained constant as the CBD dose increased; 0.5 μM CBD (11.08 ± 1.688 mpH/min) ($p<0.01$), 1 μM CBD (10.29 ± 0.9141 mpH/min) ($p<0.001$), 2.5 μM CBD (11.19 ± 1.496 mpH/min) ($p<0.01$), 5 μM CBD (11.03 ± 1.390 mpH/min) ($p<0.01$) (Untreated, 16.41 ± 1.810 mpH/min).

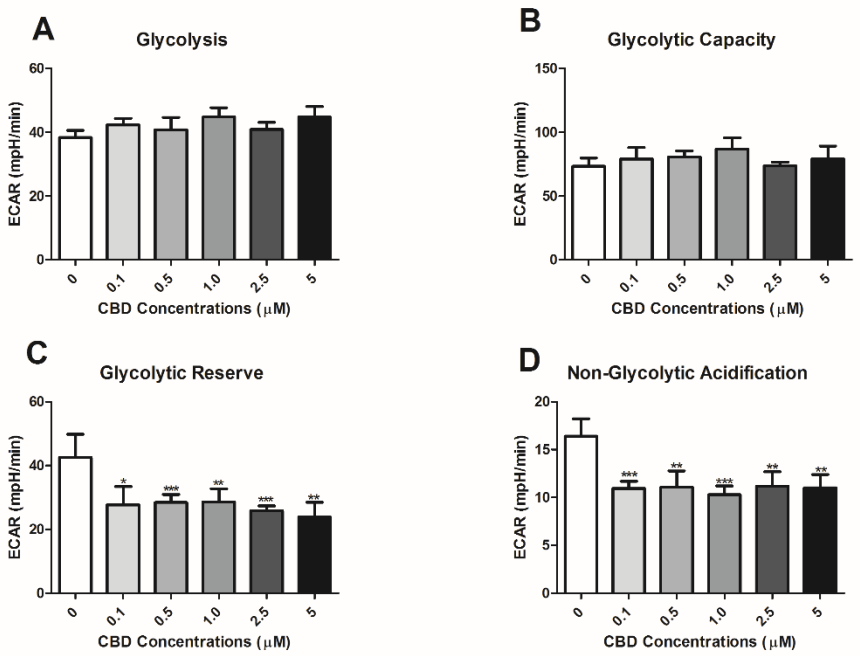

Figure 3.30. The effect of chronic CBD treatment on glycolysis in MDA-MB231 cells. Various parameters of the glycolytic mechanism were examined after 24 hours of CBD treatment with MDA-MB231 cells. **(A)** Glycolysis, **(B)** glycolytic capacity, **(C)** Glycolytic reserve and **(D)** Non-glycolytic acidification were examined. Data shown is repeated 3 times with 4 technical replicates per plate. Data is represented as mean ± SEM. *p<0.05, ** p<0.01, *** p<0.001 *vs* Untreated.

3.9.2. Glycolysis assessment following chronic CBD treatment in control Cells

Chronic treatment of control cells showed a dose dependant increase in glycolysis as CBD treatment increased (Figure 3.31.A.). There was a significant increase following treatment with 0.1 μM CBD (47.99 ± 3.248 mpH/min) (p<0.05), 0.5 μM CBD (54.28 ± 4.347 mpH/min) (p<0.01), 1 μM CBD (56.74 ± 3.113 mpH/min) (p<0.01), 2.5 μM CBD (66.19 ± 4.946 mpH/min) (p<0.01) and 5 μM CBD (62.69 ± 4.500 mpH/min) (p<0.01) (Untreated, 40.10 ± 2.315 mpH/min). Glycolytic capacity was significantly reduced with 0.1 μM CBD (84.00 ± 8.143 mpH/min) (p<0.05) (Figure 3.31.B.). This reduction continued in a dose dependant manner as CBD treatment increased; 0.5 μM CBD (72.57 ± 4.076 mpH/min) (p<0.01), 1 μM CBD (72.43 ± 7.351 mpH/min) (p<0.01), 2.5 μM CBD (66.34 ± 9.118 mpH/min) (p<0.01), 5 μM CBD (60.17 ± 11.52 mpH/min)

(p<0.01) (Untreated, 103.5 ±9.565 mpH/min). Furthermore, glycolytic reserve was trending to decrease slightly as doses of CBD increased; 0.1 μM CBD (52.65 ± 4.174 mpH/min) (p<0.05), 0.5 μM CBD (54.96 ± 3.664 mpH/min) (p<0.05), 1 μM CBD (48.54 ± 5.532 mpH/min) (p<0.01), 2.5 μM CBD (60.94 ± 6.953 mpH/min) (p=0.1), 5 μM CBD (54.89 ± 5.871 mpH/min) (p<0.05) (Untreated, 73.39 ± 6.543 mpH/min) (Figure 3.31.C.). Interestingly, when control cells were analysed for non-glycolytic acidification rates there was a significant reduction following treatment with 0.1 μM CBD (6.167 ± 0.5702 mpH/min) (p<0.001) (Figure 3.31.D.). This significant reduction trended to increase as the doses of CBD increased; 0.5 μM CBD (6.70 ± 0.982 mpH/min) (p<0.001), 1 μM CBD (7.0 ± 0.59 mpH/min) (p<0.001), 2.5 μM CBD (8.11 ± 1.40 mpH/min) (p<0.05) (Untreated, 12.39 ± 0.691 mpH/min). Moreover, there was no significant difference with 5 μM CBD.

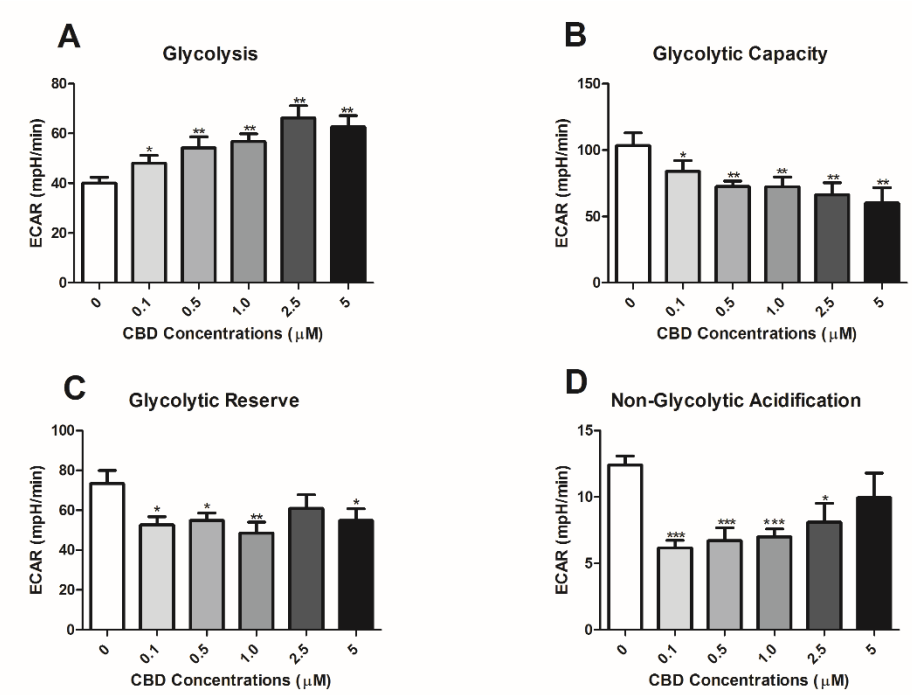

Figure 3.31. The effect of chronic CBD treatment on the glycolysis of control cells. Control cells glycolysis was measured after 24 hours of CBD treatment. **(A)** Glycolysis, **(B)** glycolytic capacity, **(C)** glycolytic reserve and **(D)** non-glycolytic acidification was examined compared to untreated cells. Data shown is repeated 3 times with 4 technical replicates per plate. Data is represented as mean ± SEM. *p<0.05, **p<0.01, *** p<0.001 *vs* Untreated.

3.10. The mitochondrial receptor, VDAC1's, response to chronic CBD treatment

CBD has been previously shown to interact with and regulate the VDAC1 channel (Section 1.4.4.) (Rimmerman *et al.* 2013). The VDAC1 channel has been linked with controlling metabolite trafficking and apoptosis within the cell (Madesh and Hajnóczky 2001, Shoshan-Barmatz *et al.* 2010, Huang *et al.* 2013). VDAC1 concentrations were analysed using western blot (Section 2.14.).

3.10.1. The effect of chronic CBD treatment on VDAC1 expression in cancer cells

Chronic treatment with CBD increased VDAC1 protein expression following 0.1 μM CBD (1.64 ± 0.104 R.I.) ($p<0.01$) treatment compared to untreated levels (Figure 3.32.A). This increase remained with 0.5 μM CBD (1.53 ± 0.156 R.I.) ($p<0.05$) and 1 μM CBD (1.45 ± 0.111 R.I.) ($p<0.05$). However, as the dose of CBD increased further VDAC1 expression trended to decrease to expression levels similar to untreated levels.

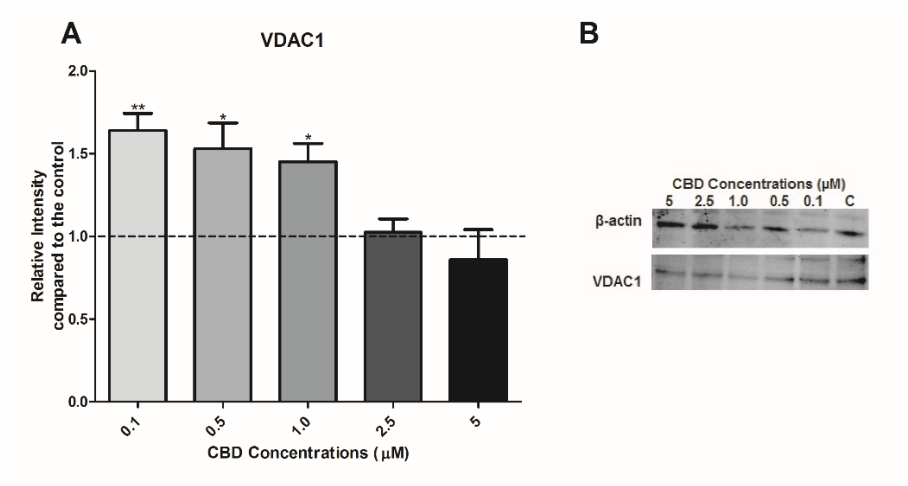

Figure 3.32. The effect of chronic CBD treatment on VDAC1 protein expression levels in cancer cells.
(A) Protein samples were analysed for changes in VDAC1 expression following CBD treatment in cancer cells. Data shown is repeated 3-5 times with the dashed line representing untreated levels. **(B)** Western blot of relevant graphs with untreated (C) and protein control of β-actin. Data is represented as mean ± SEM. *$p<0.05$, **$p<0.01$ *vs* Untreated.

3.10.2. The effect of chronic CBD treatment on VDAC1 receptor expression levels in control cells

A significant reduction in VDAC1 protein expression levels was observed following 0.5 μM CBD (0.88 ± 0.034 R.I.) ($p<0.05$) treatment (Figure 3.33.A.). This effect continued as concentrations of CBD increased; 1 μM CBD (0.79 ± 0.022 R.I.) ($p<0.001$), 2.5 μM CBD (0.84 ± 0.029 R.I.) ($p<0.01$), 5 μM CBD (0.81 ± 0.065 R.I.) ($p<0.05$).

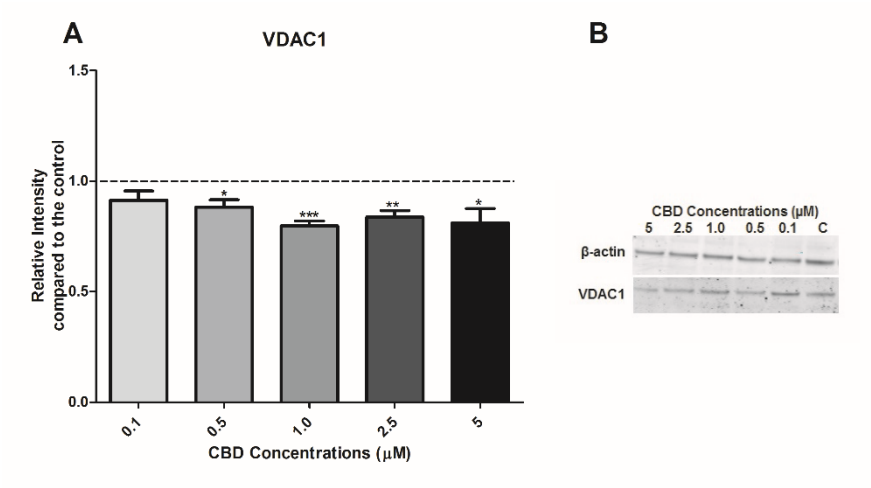

Figure 3.33. The effect of chronic CBD treatment on VDAC1 protein expression of control cells.
(A) Control cells VDAC1 changed were measured and compared to untreated levels. Data shown is repeated 3-5 times with the dashed line representing untreated levels. **(B)** Western blot of relevant graphs with untreated (C) and protein control of β-actin. Data is represented as mean ± SEM. *$p<0.05$, **$p<0.01$, *** $p<0.001$ *vs* Untreated.

3.11. The assessment of genetic changes in the cell following chronic CBD treatment

The changes observed with the metabolism of the cell following CBD treatment indicated that there could be some pivotal changes occurring within the regulation of the cell at a genetic level. Several key pathways were targeted that control cell growth and apoptosis. The pro-apoptotic p53 pathway was selected along with activators of p53, HDAC1 and SirT1 (Section 1.4.3.). Nrf2 has been shown to regulate ROS activity and cellular stress therefore alterations to its mechanism was important to measure (Section 1.1.3.4.1.) (Kensler *et al.* 2007). Finally the cell growth regulator AKT was also analysed along with its targets, mTOR and NFκB. These pathways were analysed by qPCR and normalised to the relevant housekeeping gene (Section 2.12.).

3.11.1. The effect of chronic CBD treatment on gene expression in cancer cells

3.11.1.1. Chronic CBD's effect on the p53 pathway and its regulation

The pro-apoptotic p53 pathway was selected as it is a master regulator of apoptosis (Ito *et al.* 2002, Bansal *et al.* 2011, Wade *et al.* 2013). HDAC1 has been linked to deacetylation of p53 which activates cellular growth and inhibits apoptosis (Luo *et al.* 2000, Ito *et al.* 2002). Whereas SirT1 has been shown to have anti-tumourogenic properties while in parallel activates p53 and translocates activated p53 to the mitochondrial to induce intrinsic apoptotic cell death (Yi and Luo 2010, Tan *et al.* 2014).

A significant decrease in HDAC1 gene expression was observed following chronic treatment with all doses of CBD; 0.1 μM (1.28 ± 0.273 R.I.) ($p<0.001$), 0.5 μM CBD (1.34 ± 0.093 R.I.) ($p<0.05$), 1 μM CBD (1.53 ± 0.103 R.I.) ($p<0.05$), 2.5 μM CBD (1.71 ± 0.136 R.I.) ($p<0.05$), 5 μM CBD (1.75 ± 0.273 R.I.) ($p<0.05$) (Figure 3.34.A.). This decrease remained constant and no change was observed between treatments.

There was a significant increase in SirT1 expression levels following 0.1 μM CBD (385.2 ± 117.21 R.I.) ($p<0.05$) treatment (Figure 3.34.B.). This increase followed a dose dependant increase as CBD dose increased; 0.5 μM CBD (531.0 ± 123.12 R.I.) ($p<0.05$), 1 μM CBD (586.0 ± 140.22 R.I.) ($p<0.05$), 2.5 μM CBD (620.2 ± 38.49 R.I.) ($p<0.001$), 5 μM CBD (648.2 ± 56.56 R.I.) ($p<0.01$).

Following chronic CBD treatment p53 gene expression showed a trend to increase compared to untreated levels (Figure 3.34.C.). This reached significance following treatment with 0.5 μM CBD (1.34 ± 0.093 R.I.) ($p<0.05$), 1 μM CBD (1.53 ± 0.103 R.I.) ($p<0.05$), 2.5 μM CBD (1.71 ± 0.136 R.I.) ($p<0.05$), 5 μM CBD (1.75 ± 0.273 R.I.) ($p<0.05$).

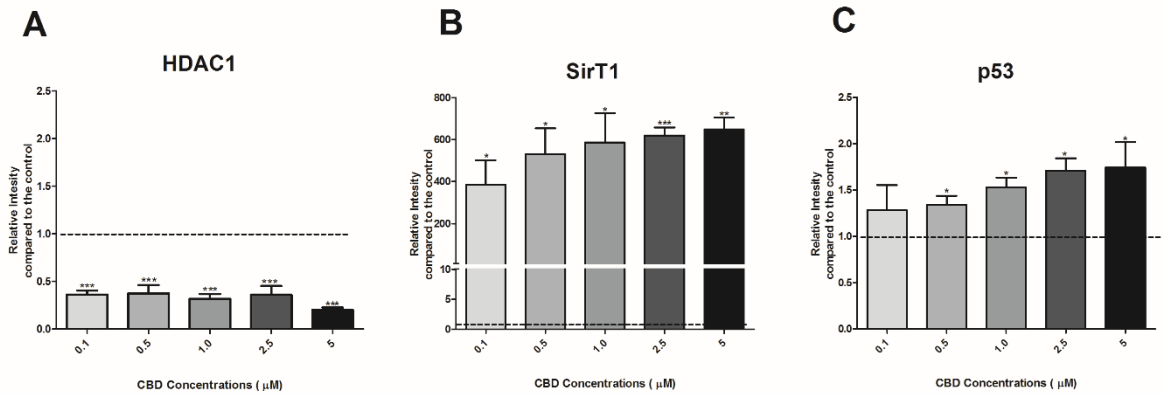

Figure 3.34. The effect of chronic CBD treatment on the gene expression of the p53 pathway in cancer cells.
Cancer cell's mRNA was examined for any alteration to the p53 pathway. **(A)** HDAC1, **(B)** SirT1 and **(C)** p53, gene expression levels were analysed after mRNA extraction. Data shown is repeated 3-5 times with the dashed line representing untreated levels. Data is represented as mean ± SEM. *$p<0.05$, **$p<0.01$, *** $p<0.001$ *vs* Untreated.

3.11.1.2. The Nrf2 pathway's response to chronic CBD treatment in cancer cells

A key regulator of ROS is Nrf2 which can be regulated directly through Nrf2's binding with KEAP1 (Section 1.1.3.4.1.) (Kensler *et al.* 2007). An increase in ROS leads

to Nrf2 being liberated from Nrf2. This liberation can also be regulated by increased inflammation such as with MAPκ (Jeong *et al.* 2006). MAPκ can regulate Nrf2 and IL-6 activity (Son *et al.* 2008).

The cellular stress response pathway of Nrf2 showed an increase in MAPκ expression activity compared to untreated levels. This reached a significant increase following treatment with 0.1 μM CBD (78.20 ± 2.565 R.I.) ($p<0.05$) (Figure 3.35.A.). This effect increased in a dose dependant manner; 0.5 μM CBD (93.36 ± 4.991 R.I.) ($p<0.01$), 1 μM CBD (112.0 ± 5.14 R.I.) ($p<0.01$), 2.5 μM CBD (150.4 ± 11.59 R.I.) ($p<0.05$), 5 μM CBD (195.3 ± 20.96 R.I.) ($p<0.05$).

Nrf2 gene expression levels also had a trend to increase in expression compared to untreated cells (Figure 3.35.B.). This reached significance following treatment with 1 μM CBD (2.49 ± 0.289 R.I.) ($p<0.05$) and continued in a dose dependant increase as CBD doses increased; 2.5 μM CBD (3.77 ± 0.376 R.I.) ($p<0.05$), 5 μM CBD (6.25 ± 0.512 R.I.) ($p<0.01$).

There was a significant increase in IL-6 expression, an anti-inflammatory marker, following 0.1 μM CBD (6.62 ± 1.099 R.I.) ($p<0.05$) treatment (Figure 3.35.C.). As CBD dose increased, a dose dependant increase was observed; 0.5 μM CBD (7.49 ±1.904 R.I.) ($p<0.05$), 1 μM CBD (10.99 ± 1.849 R.I.) ($p<0.05$), 2.5 μM (13.03 ± 3.699 R.I.) ($p<0.05$), 5 μM CBD (15.06 ± 2.151 R.I.) ($p<0.05$).

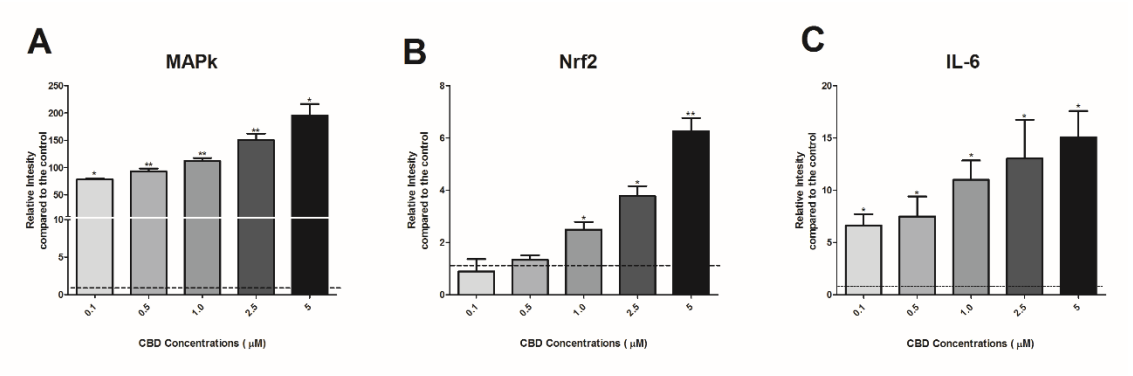

Figure 3.35. The effect of chronic CBD treatment on the Nrf2 pathway's gene expression in cancer cells.
Cancer cell's Nrf2 pathway was examined for alterations to gene expression after chronic CBD treatment. **(A)** MAPκ, **(B)** Nrf2 and **(C)** IL-6 gene expression levels were analysed after mRNA extraction. Data shown is repeated 3-5 times with the dashed line representing untreated levels. Data is represented as mean ± SEM. *p<0.05, **p<0.01, *** p<0.001 *vs* Untreated.

3.11.1.3. The effect on gene expression of the AKT pathway following chronic CBD treatment

The regulation of cellular growth and metabolism has been linked to mTOR and AKT activity (Sarbassov *et al.* 2005, Humphrey *et al.* 2013, Liu *et al.* 2013). These regulators have been shown to be over expressed in cancer cells which suggests they could play an important role in cancer cell regulation (Humphrey *et al.* 2013). Furthermore, NFκB is known to inhibit apoptosis and promote cell growth (Nakanishi and Toi 2005).

AKT gene expression levels showed a trend to increase compared to untreated levels (Figure 3.36.A.). However, there was no significant alteration to gene expression.

There was a significant increase in mTOR expression following chronic CBD treatment with 0.1 μM CBD (6.81 ± 1.096 R.I.) ($p<0.05$) (Figure 3.36.B.). As the dose of CBD increased, a dose dependant decrease in mTOR expression was observed; 0.5 μM CBD (4.98 ± 0.910 R.I.) ($p<0.05$), 1 μM CBD (2.55 ± 0.303 R.I.) ($p<0.05$). When the dose of CBD reached 2.5 μM CBD and 5 μM CBD there was no further difference to untreated levels.

NFκB expression levels showed an increase in expression levels compared to untreated cells (Figure 3.36.C.). This reached a significant increase following treatment with 1 μM CBD (2.40 ± 0.221 R.I.) ($p<0.05$), 2.5 μM CBD (4.30 ± 0.620 R.I.) ($p<0.05$) and 5 μM CBD (6.01 ± 0.650 R.I.) ($p<0.05$).

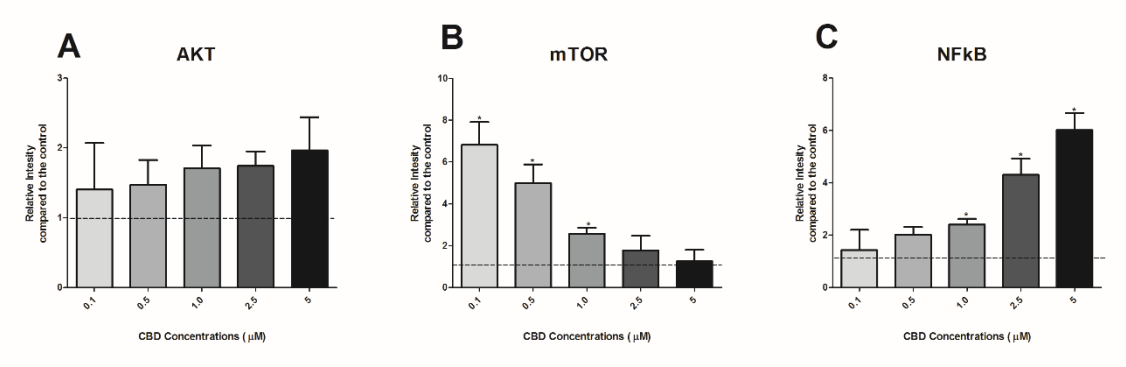

Figure 3.36. Chronic CBD's effect on the gene expression of the AKT pathway in cancer cells.
Cancer cell's mRNA was isolated and examined for AKT alterations to gene expression. **(A)** AKT, **(B)** mTOR and **(C)** NFκB gene expression levels were analysed after mRNA extraction. Data shown is repeated 3-5 times with the dashed line representing untreated levels. Data is represented as mean ± SEM. *$p<0.05$, **$p<0.01$, *** $p<0.001$ *vs* Untreated.

3.11.1.4. The effect of chronic CBD treatment on the gene expression of TNFα, FOXO1 and FOXO3 in cancer cells

Additional genes were analysed to aid in further understanding CBD's mode of action in cancer cells. Tumour necrosis factor α (Tnfα) has been implicated in inflammation and have been suggested to play a role in cancer regulation (Miles *et al.* 1994, Barbisan *et al.* 2012). Moreover, FOXO activity has been shown to suppress oxidative stress and inhibit cancer growth (Nunn *et al.* 2010, Jiang *et al.* 2013). These additional regulators of cancer cell growth were included in the investigation of the molecular mechanism of "priming" with CBD.

There was a trend to increase of TNFα gene expression compared to untreated (Figure 3.37.A.). However, no significant alteration was observed.

A dose dependent increase in FOXO1 cancer cell gene expression was observed following CBD treatment from 0.1 μM (33.79 ± 8.228 R.I.) ($p<0.05$), 0.5 μM CBD (31.44 ± R.I.) ($p<0.05$), 1 μM CBD (33.79 ± 9.896 R.I.) ($p<0.05$), 2.5 μM CBD (43.66 ± 7.618 R.I.) ($p<0.05$) and 5 μM CBD (47.91 ± 10.241 R.I.) ($p<0.05$) (Figure 3.37.B.).

Interestingly following chronic CBD treatment, a decrease in FOXO3 gene expression was observed with 0.1 μM CBD (0.23 ± 0.059 R.I.) ($p<0.01$) treatment (Figure 3.37.C.). This decrease initially observed had a trend to increase, in a dose-dependent manner towards untreated levels as the dose of CBD increased; 0.5 μM CBD (0.44 ± 0.068 R.I.) ($p<0.05$), 1 μM CBD (0.43 ± 0.071 R.I.) ($p<0.05$), 2.5 μM CBD (0.64 ± 0.029 R.I.) ($p<0.01$) and 5 μM CBD (0.64 ± 0.050 R.I.) ($p<0.05$).

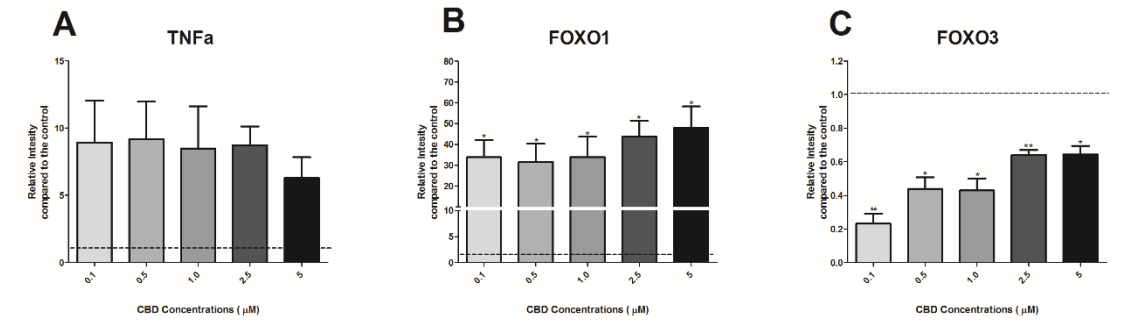

Figure 3.37. The gene expression of cancer cells TNFα, FOXO1 and FOXO3 following chronic CBD treatment.
Cancer cell's **(A)** TNFa, **(B)** FOXO1 and **(C)** FOXO3 were examined after chronic CBD treatment. Data shown is repeated 3-5 times with the dashed line representing untreated levels. Data is represented as mean ± SEM. *$p<0.05$, **$p<0.01$, *** $p<0.001$ *vs* Untreated.

3.11.2. The effect of chronic CBD treatment on the gene expression of control cell

3.11.2.1. The effect to p53 pathway's gene expression following chronic CBD treatment in control cells.

Within the p53 pathway, a dose dependant increase in HDAC1 gene expression following CBD treatment was observed (Figure 3.38.A.). This reached significance following treatment with 0.1 μM CBD (1.66 ± 0.159 R.I.) ($p<0.05$), 0.5 μM CBD (1.73 ±

0.223 R.I.) (p<0.05), 1 μM CBD (2.28 ± 0.313 R.I.) (p<0.05), 2.5 μM CBD (3.59 ± 0.772 R.I.) (p<0.05), 5 μM CBD (3.70 ± 0.833 R.I.) (p<0.05).

SirT1 gene expression was significantly reduced following treatment with 0.1 μM CBD (0.49 ± 0.042 R.I.) (p<0.01) (Figure 3.38.B.). However, as CBD dose increased a trend to increase in a dose dependant manner was observed. This reached a significant increase compared to untreated cells at 2.5 μM CBD (2.09 ± 0.159 R.I.) (p<0.05) and 5 μM CBD (3.91 ± 0.274 R.I.) (p<0.01).

A similar effect was observed following CBD treatment in p53 gene expression (Figure 3.38.C.) A significant reduction in gene expression was observed following treatment with 0.1 μM CBD (0.36 ± 0.062 R.I.) (p<0.01) which was lost as CBD doses increased to finally level with untreated cells. There was a significant increase in expression levels following treatment with 2.5 μM CBD (1.46 ± 0.149 R.I.) (p<0.05) and 5 μM CBD (1.95 ± 0.354 R.I.) (p<0.05).

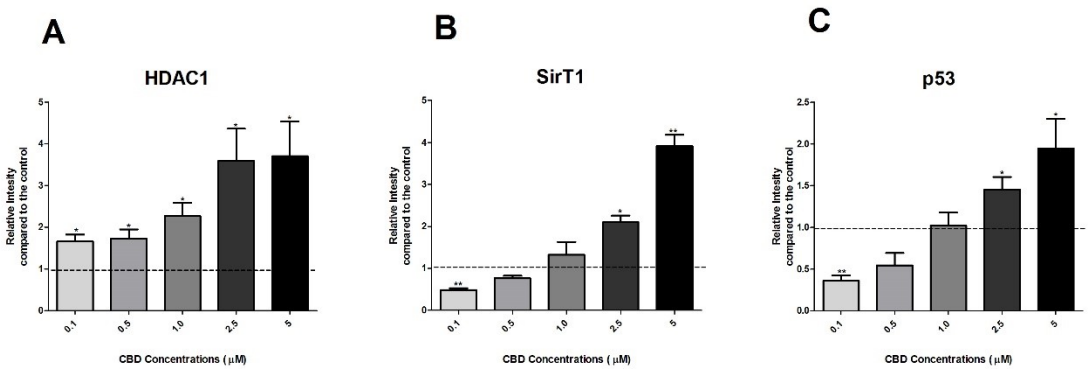

Figure 3.38. The effect of chronic CBD treatment on the gene expression of the p53 pathway in control cells.
Gene expression levels were analysed for any alterations to the p53 pathway. **(A)** HDAC1, **(B)** SirT1 and **(C)** p53 were analysed after mRNA extraction. Data shown is repeated 3-5 times with the dashed line representing untreated levels. Data is represented as mean ± SEM. *p<0.05, **p<0.01 *vs* Untreated.

3.11.2.2. Chronic CBD's effect on the gene expression of the Nrf2 pathway

When the Nrf2 pathway was examined a significant decrease in MAPк was observed following treatment with 0.1 μM CBD (0.42 ± 0.064 R.I.) ($p<0.05$) (Figure 3.39.A.). This decrease showed a dose dependant trend to increase as CBD dose increased; 0.5 μM CBD (0.35 ± 0.067 R.I.) ($p<0.05$), 1 μM CBD (0.43 ± 0.105 R.I.) ($p<0.05$) and 2.5 μM CBD (0.76 ± 0.034 R.I.) ($p<0.05$). There was no significant change compared to untreated cells when the highest dose of CBD was reached, 5 μM CBD.

Nrf2 gene expression also showed a dose dependant trending increased with increased CBD treatment (Figure 3.39.B.). This reached significant expression at 2.5 μM CBD (3.10 ± 0.735 R.I.) ($p<0.05$) and 5 μM CBD (4.88 ± 1.167 R.I.) ($p<0.05$).

A dose dependant increase was also observed with IL-6 gene expression following CBD treatment (Figure 3.39.C.). A significant increase was observed with 2.5 μM CBD (1.19 ± 0.013 R.I.) ($p<0.05$) and 5 μM CBD (1.41 ± 0.079 R.I.) ($p<0.05$).

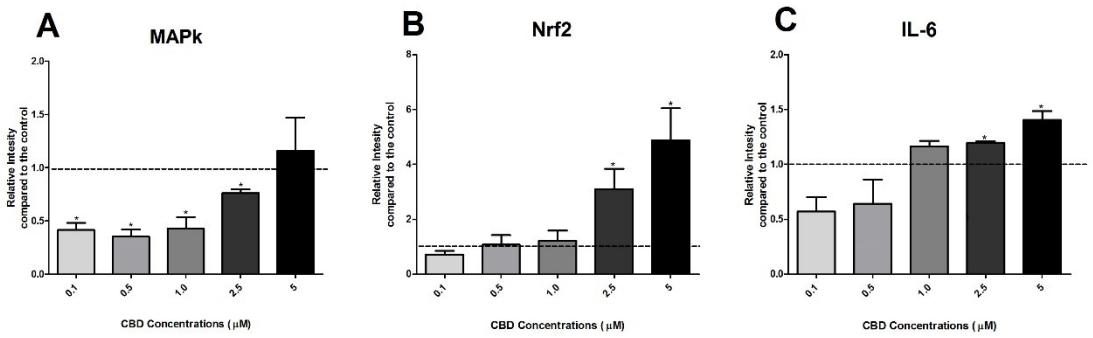

Figure 3.39. The effect of chronic CBD treatment on the Nrf2 pathway's gene expression in control cells.
Gene expression levels of the Nrf2 pathway were analysed with normal cells. **(A)** MAPк, **(B)** Nrf2 and **(C)** IL-6 gene expression levels were analysed after mRNA extraction. Data shown is repeated 3-5 times with the dashed line representing untreated levels. Data is represented as mean ± SEM. *$p<0.05$, **$p<0.01$, *** $p<0.001$ *vs* Untreated.

3.11.2.3. AKT Pathway

AKT expression showed a dose dependant trend to increase as CBD treatment increased (Figure 3.40.A.). A significant increase was reached following treatment with 2.5 μM CBD (2.45 ± 0.497 R.I.) ($p<0.05$) and 5 μM CBD (4.03 ± 0.738 R.I.) ($p<0.05$).

mTOR gene expression activity also showed a dose dependant trend to increase compared to untreated levels (Figure 3.40.B.). This reached a significant increase following treatment with 5 μM CBD (2.31 ± 0.189 R.I.) ($p<0.05$).

There was a differing response with NFκB expression as an initial increase in gene expression was observed following treatment with 0.1 μM CBD (2.21 ± 0.257 R.I.) ($p<0.05$) (Figure 3.40.C.). However, as doses of CBD increased there was a trending dose dependant decrease in NFkB expression; 0.5 μM CBD (2.11 ± 0.240 R.I.) ($p<0.05$) and 1 μM CBD (1.64 ± 0.147 R.I.) ($p<0.05$). Once the dose of CBD reached 2.5 μM CBD and 5 μM CBD there was no significant difference to untreated expression levels.

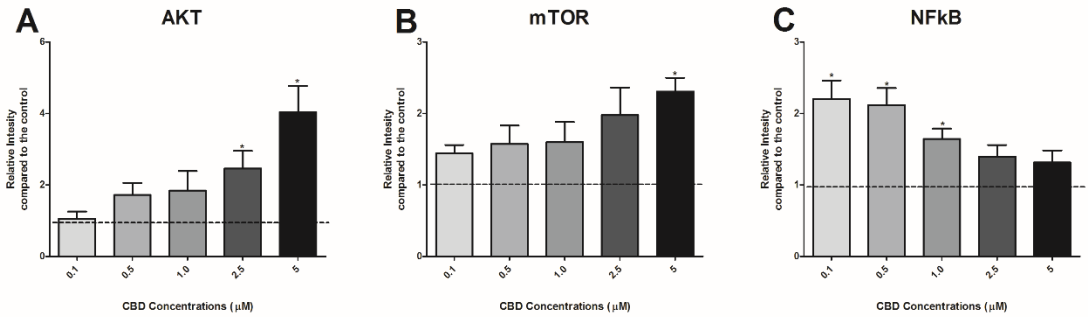

Figure 3.40. The effect of chronic CBD treatment on the gene expression of the AKT pathway in control cells.
Gene expression levels were analysed for AKT pathway alterations; **(A)** AKT, **(B)** mTOR, **(C)** NFκB, gene expression levels were analysed after mRNA extraction. Data shown is repeated 3-5 times with the dashed line representing untreated levels. Data is represented as mean ± SEM. *$p<0.05$, **$p<0.01$, *** $p<0.001$ *vs* Untreated.

3.11.2.4. Chronic CBD's effect on the gene expression of TNFα, FOXO1 and FOXO3 in control cells

Following chronic treatment with CBD, TNFα showed an increase in expression which reached significance following treatment with 1 μM CBD (3.15 ± 0.169 R.I.) ($p<0.01$), 2.5 μM CBD (3.51 ± 0.209 R.I.) ($p<0.01$), 5 μM CBD (3.80 ± 0.073 R.I.) ($p<0.001$) (Figure 3.41.A.).

FOXO1 also showed a dose dependant increased response to increased CBD treatment (Figure 3.41.B.). A significant increase was reached following treatment with 0.5 μM CBD (1.79 ± 0.146 R.I.) ($p<0.05$), 1 μM CBD (2.07 ± 0.294 R.I.) ($p<0.05$), 2.5 μM CBD (2.88 ± 0.441 R.I.) ($p<0.05$), 5 μM CBD (3.55 ± 0.367 R.I.) ($p<0.05$).

Furthermore, FOXO3 showed a dose dependent trend to increase in gene expression as treatment of CBD increased (Figure 3.41.C.). This reached a significant expression increase following treatment with 2.5 μM CBD (3.81 ± 0.374 R.I.) ($p<0.05$) and 5 μM CBD (5.58 ± 0.823 R.I.) ($p<0.05$).

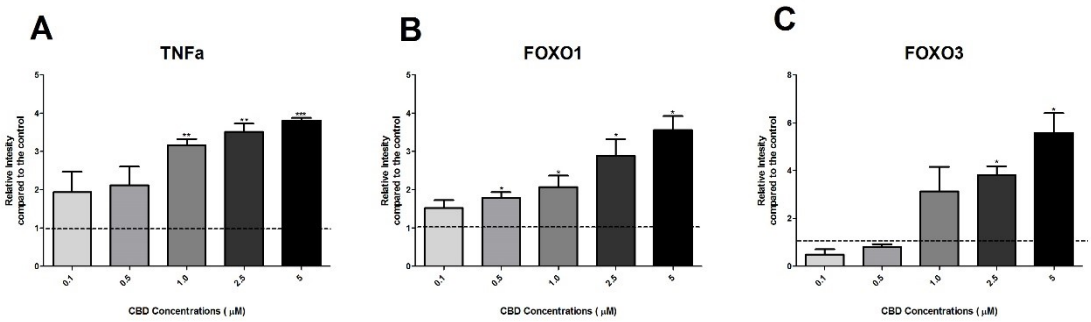

Figure 3.41. Chronic CBD's effect on the gene expression of TNFα, FOXO1 and FOXO3 in control cells.
Gene expression levels were analysed with normal cells for **(A)** TNFα, **(B)** FOXO1 and **(C)** FOXO3 gene expression levels were analysed after mRNA extraction. Data shown is repeated 3-5 times with the dashed line representing untreated levels. Data is represented as mean ± SEM. *$p<0.05$, **$p<0.01$, *** $p<0.001$ *vs* Untreated.

3.12. Following chronic CBD treatment protein level was analysed

The alterations observed with gene expression analysis led to further protein level concentration examination on the same pathways as described in section 3.11.. This analysis was carried out using western blotting (Section 2.13.).

3.12.1. The effect following chronic CBD treatment on cancer cells protein levels

Cells were treated with CBD for 24 hours prior to harvesting for protein analysis. A certain set of pathways was analysed for alteration in protein expression. The p53 pathway which includes, HDAC1, SirT1 and p53 (Section 3.11.1.1.). The cell stress response pathway of Nrf2 which consisted of HDAC6, Nrf2 and IL-6 (Section 3.11.1.2.). Finally, the growth pathway of AKT: AKT1, global AKT, mTOR and NFκB (Section 3.11.1.3.).

3.12.1.1. Chronic CBD's treatment effect on the protein levels of p53 pathway in cancer cells

Following chronic treatment with CBD, cancer cell's HDAC1 levels were overexpressed compared to untreated protein levels (Figure 3.42.A.). A significant increase in protein level of HDAC1 was observed; 0.1 μM CBD (1.74 ± 0.148 R.I.) ($p<0.05$), 0.5 μM CBD (1.59 ± 0.059 R.I.) ($p<0.05$), 1 μM CBD (1.89 ± 0.081 R.I.) ($p<0.01$), 2.5 μM CBD (1.85 ± 0.159 R.I.) ($p<0.05$), 5 μM CBD (1.81 ± 0.126 R.I.) ($p<0.05$). This increase remained constant throughout the increased CBD treatment.

SirT1 protein levels were increased following chronic treatment with 0.1 μM CBD (1.46 ± 0.085 R.I.) ($p<0.01$) and 0.5 μM CBD (1.38 ± 0.158 R.I.) ($P<0.05$) (Figure 3.42.B.). However, as the dose of CBD increased a trend to decrease was observed.

This decrease reached significance following treatment with 5 μM CBD (0.54 ± 0.087 R.I.) ($p<0.01$).

There was an increase in p53 levels following chronic CBD treatment that had a trend to increase with increased CBD dose (Figure 3.42.C.). This increase began following treatment with 0.1 μM CBD (1.96 ± 0.257 R.I.) ($p<0.05$), 0.5 μM CBD (2.38 ± 0.411 R.I.) ($p<0.05$), 1 μM CBD (2.27 ± 0.310 R.I.) ($p<0.05$), 2.5 μM CBD (2.64 ± 0.510 R.I.) ($p<0.05$) and 5 μM CBD (2.26 ± 0.359 R.I.) ($p<0.05$).

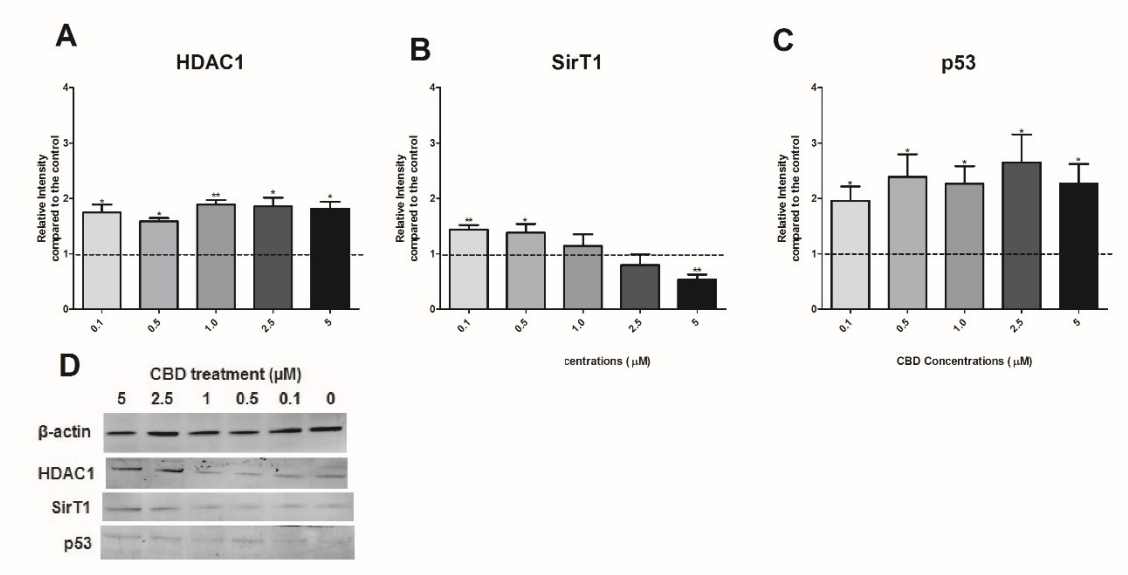

Figure 3.42. The effect of chronic CBD treatment on the protein levels of the p53 pathway in cancer cells.
Cancer cell's protein profiles were completed for the p53 pathway after 24 hours of CBD treatment. **(A)** HDAC1, **(B)** SirT1 and **(C)** p53 were analysed. **(D)** Western blot of relevant graphs with untreated (0) and the housekeeper β-actin as control protein. Data shown is repeated 3-5 times with the dashed line representing untreated levels. Data is represented as mean ± SEM. *$p<0.05$, **$p<0.01$, *** $p<0.001$ *vs* Untreated.

3.12.1.2. The effect of chronic CBD treatment on the protein levels of the Nrf2 pathway in cancer cells

Following chronic CBD treatment there was no change in HDAC6 protein levels compared to untreated cells (Figure 3.43.A.). As the dose of CBD increased the protein level was unchanged compare to untreated cells.

There was a significant dose dependant increase in Nrf2 protein levels as CBD treatment increased (Figure 3.43.B.). This increase reached significance following treatment with 0.5 μM CBD (1.67 ± 0.102 R.I.) ($p<0.05$), 1 μM CBD (2.43 ± 0.291 R.I.) ($p<0.01$), 2.5 μM CBD (2.84 ± 0.505 R.I.) ($p<0.05$) and 5 μM CBD (3.30 ± 0.545 R.I.) ($p<0.05$).

When the IL-6 protein levels were measured following chronic CBD treatment, no change was observed (Figure 3.43.C.). The levels of IL-6 remained similar to untreated levels.

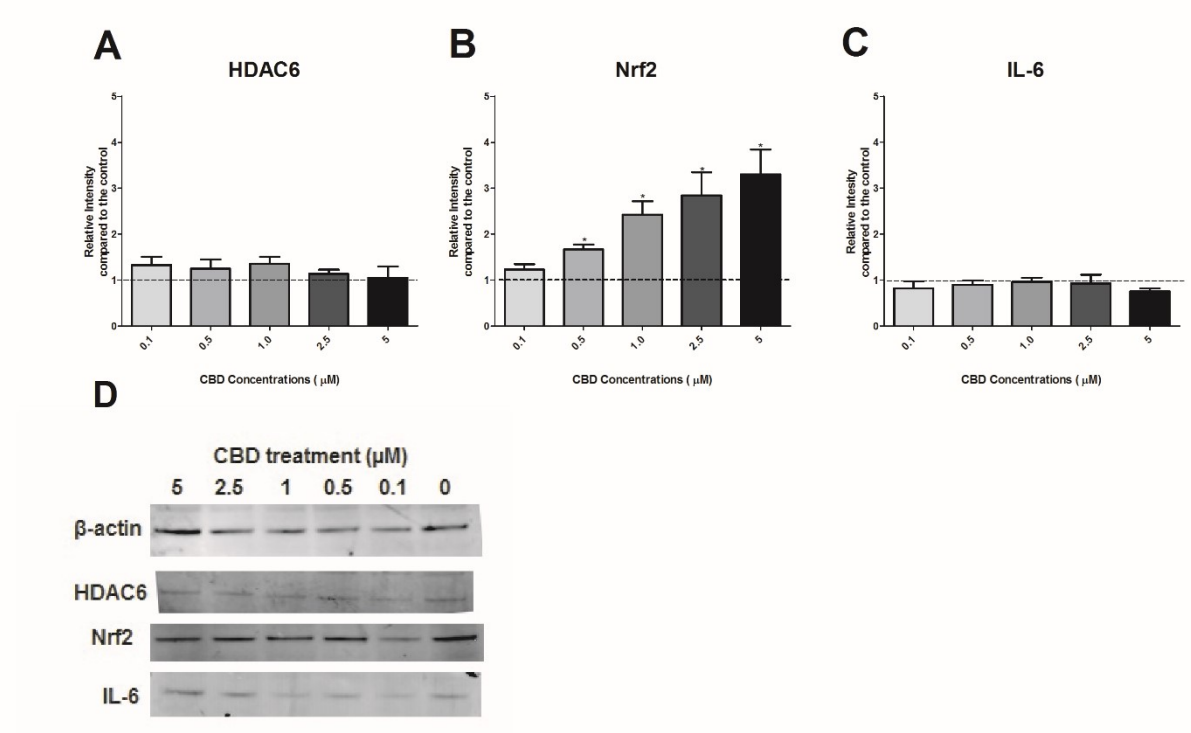

Figure 3.43. The effect of chronic CBD treatment on the protein levels of the Nrf2 pathway in cancer cells.
Cancer cells had their protein profiles completed for the Nrf2 pathway after chronic CBD treatment. **(A)** HDAC6, **(B)** Nrf2 and **(C)** IL-6 protein expression levels were examined compared to untreated cells. Data shown is repeated 3-5 times with the dashed line representing untreated levels. **(D)** Western blot of relevant graphs with untreated (0) and the housekeeper β-actin as control protein. Data is represented as mean ± SEM. *$p<0.05$, **$p<0.01$, *** $p<0.001$ *vs* Untreated.

3.12.1.3. The effect of chronic CBD treatment on the protein levels of the AKT pathway in cancer cells.

AKT1 protein levels were measured following chronic CBD treatment (Figure 3.44.A.). There was a slight dose dependant trend to increase in AKT1 protein levels. However, these were not significant and remained similar to untreated levels.

Thus, the global levels of AKT were analysed following CBD treatment (Figure 3.44.B.). An increase in protein levels were observed following treatment with 0.1 μM CBD (1.78 ± 0.172 R.I.) ($p<0.05$). Interestingly though, this increase did not remain and there was a trend to decrease of global AKT protein levels in the cells. This reached a significant reduction following treatment with 5 μM CBD (0.44 ± 0.126 R.I.) ($p<0.05$).

mTOR protein levels were measured to complete the mode of action of CBD in the AKT pathway. An increase in mTOR levels was observed following treatment with 0.1 μM CBD (1.98 ± 0.192 R.I.) ($p<0.01$) (Figure 3.44.D.). This increase remained with 0.5 μM CBD (1.87 ± 0.127 R.I.) ($p<0.01$) and 1 μM CBD treatment (1.49 ± 0.171 R.I.) ($p<0.05$). Additionally, there was a trend to decrease of mTOR protein levels as the dose of CBD increased. With 2.5 μM CBD treatment the mTOR levels were similar to untreated levels.

Examining NFκB protein levels revealed no changes compared to untreated levels (Figure 3.44.D.). However, as the dose of CBD increased a trend to decrease was observed that did not reach significance.

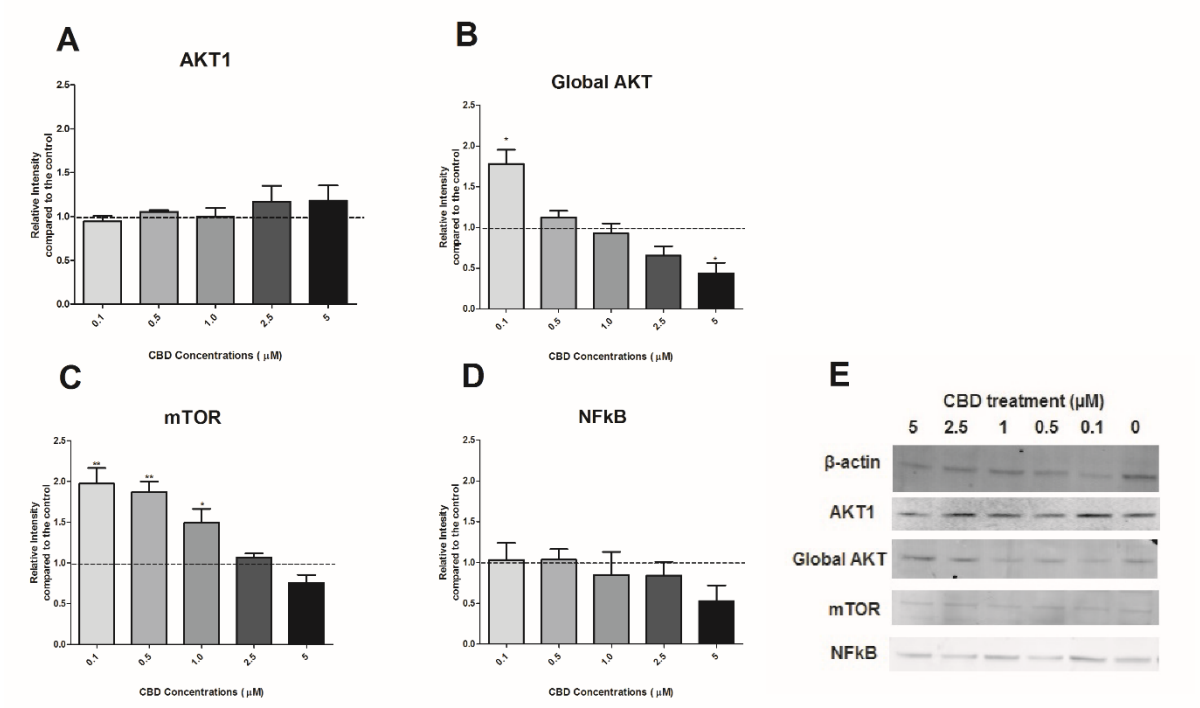

Figure 3.44. The effect of chronic CBD treatment on the protein levels of the AKT pathway in cancer cells.
Cancer cells had their protein profiles completed for the AKT pathway after chronic CBD treatment. **(A)** AKT1, **(B)** Global AKT, **(C)** mTOR and **(D)** NFκB protein expression levels were examined compared to untreated cells. **(E)** Western blot of relevant graphs with untreated (0) and the housekeeper β-actin as control protein. Data shown is repeated 3-5 times with the dashed line representing untreated levels. Data is represented as mean ± SEM. *p<0.05, **p<0.01, *** p<0.001 *vs* Untreated.

3.12.2. Chronic CBD's effect on the protein levels in control cells

Control cell's protein was extracted and analysed after chronic CBD treatment. The same pathways as described in 3.12.1. were examined.

3.12.2.1. The effect of chronic CBD treatment on the protein levels in the p53 pathway examined in control cells

Following chronic CBD treatment a trend to increase in protein levels of HDAC1 was observed (Figure 3.45.A.). However, there was no difference compared to untreated cell levels.

SirT1 levels had a dose dependant increase compared to untreated levels when treated with increasing doses of CBD. A significant increase in SirT1 levels was reached following 1 μM CBD treatment (1.62 ± 0.141 R.I.) ($p<0.01$) (Figure 3.45.B.). The increase continued to elevate as doses of CBD increased; 2.5 μM CBD (1.77 ± 0.137 R.I.)($p<0.01$), 5 μM CBD (1.94 ± 0.331 R.I.) ($p<0.05$).

There was a significant reduction in p53 levels following treatment with 0.1 μM CBD (0.82 ± 0.009 R.I.) ($p<0.001$) (Figure 3.45.C.). However, as doses of CBD increased there was a dose dependant trend to increase which reached a significant increase following treatment with 2.5 μM CBD (1.75 ± 0.202 R.I.) ($p<0.05$) and 5 μM CBD (2.11 ± 0.309 R.I.) ($p<0.05$).

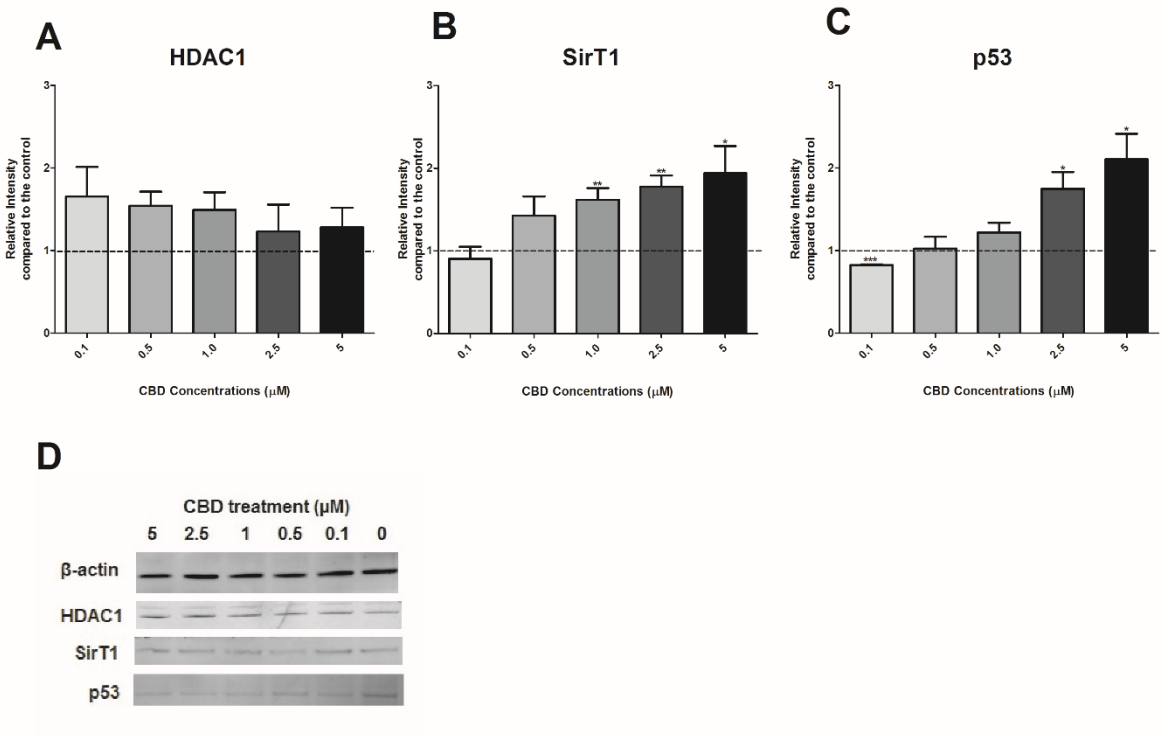

Figure 3.45. The effect of chronic CBD treatment on the protein level of the p53 pathway in control cells.
Control cells were treated with CBD for 24 hours were analysed for changes to the p53 pathway. **(A)** HDAC1, **(B)** SirT1 and **(C)** p53 protein expression levels were examined compared to untreated. **(D)** Western blot of relevant graphs with untreated (0) and the housekeeper β-actin as control protein. Data shown is repeated 3-5 times with the dashed line representing untreated levels. Data is represented as mean ± SEM. *$p<0.05$, **$p<0.01$, *** $p<0.001$ *vs* Untreated.

3.12.2.2. The chronic treatment of CBD's effect on the protein levels of the Nrf2 pathway in control cells

The Nrf2 pathway showed no change in protein levels of HDAC6 following chronic CBD treatment in the control cells (Figure 3.46.A.). There was no difference to untreated levels as CBD treatment increased.

With the chronic treatment of CBD there was also no change in Nrf2 levels within the cell (Figure 3.46.B.). The levels of Nrf2 remained similar to untreated levels with no significant alteration.

Interestingly, there was a significant increase in IL-6 levels following CBD treatment (Figure 3.46.C.). The increase was observed following treatment with 0.1 μM CBD (3.08 ± 0.063 R.I.) ($p<0.001$). This increase trended to decrease in a dose dependant manner as CBD increased; 0.5 μM CBD (3.19 ± 0.054 R.I.) ($p<0.001$), 1 μM CBD (3.22 ± 0.159 R.I.) ($p<0.01$), 2.5 μM CBD (2.97 ± 0.303 R.I.) ($p<0.05$), 5 μM CBD (2.57 ± 0.329 R.I.) ($p<0.05$).

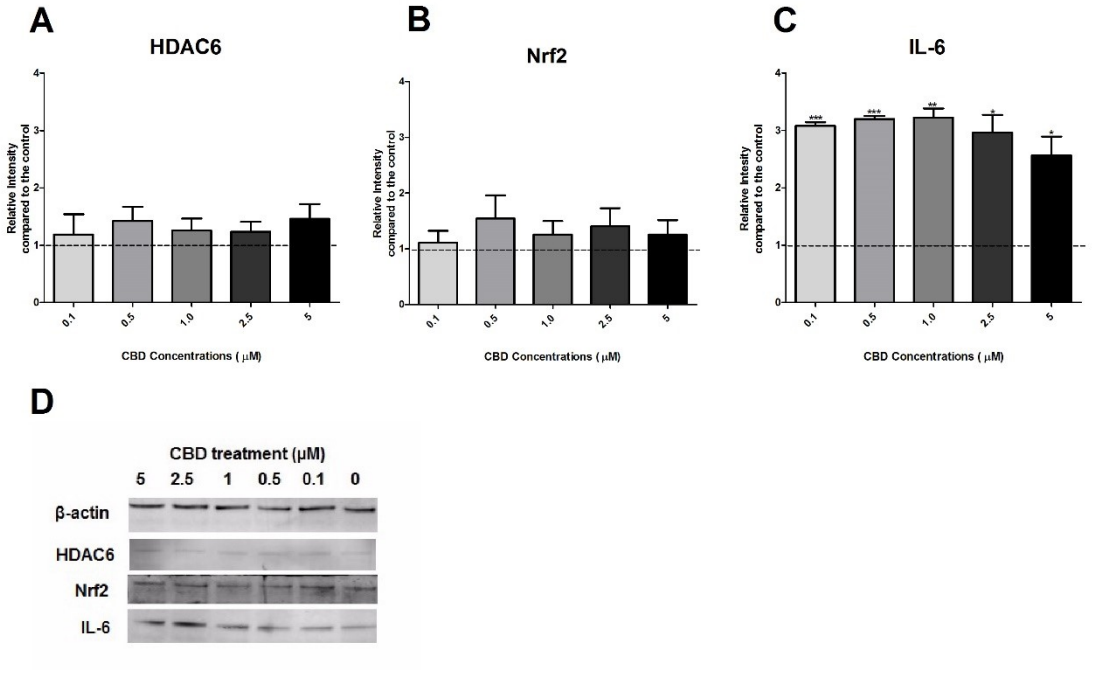

Figure 3.46. The effect of chronic CBD treatment in the protein levels of the Nrf2 pathway in control cells.
Control cells were treated with CBD for 24 hours and were examined for alterations in the Nrf2 pathway. **(A)** HDAC6, **(B)** Nrf2 and **(C)** IL-6 protein expression levels were examined compared to untreated cells. **(D)** Western blot of relevant graphs with untreated (0) and the housekeeper β-actin as control protein. Data shown is repeated 3-5 times with the dashed line representing untreated levels. Data is represented as mean ± SEM. *p<0.05, **p<0.01, *** p<0.001 *vs* Untreated.

3.12.2.3. The effect of a chronic treatment of CBD in the protein levels of the AKT pathway in control cells

Cellular growth and control is regulated in part by AKT1. There was no change in AKT1 levels compared to untreated cells (Figure 3.47.A.). The levels were very stable and similar to untreated levels.

This inhibition of alteration in AKT1 was also echoed with global AKT levels (Figure 3.47.B.). There was a trend to decrease of global AKT protein levels compared to untreated levels with all CBD doses.

NFκB protein levels were examined following chronic CBD treatment in the control cells. There was an elevation of protein levels compared to untreated following

treatment with 0.1 μM CBD (2.42 ± 0.313 R.I.) ($p<0.05$) (Figure 3.47.C.). This significant increase in NFκB levels decreased as doses of CBD increased but remained significantly increased compared to untreated levels (0.5 μM CBD, 1.65 ± 0.074 R.I., $p<0.05$; 1 μM CBD, 1.57 ± 0.113 R.I., $p<0.05$; 2.5 μM CBD, 1.43 ± 0.069 R.I., $p<0.05$; 5 μM CBD, 1.49 ± 0.102 R.I., $p<0.05$).

An increase in mTOR protein levels was also observed following treatment with 0.1 μM CBD (2.11 ± 0.288 R.I.) ($p<0.05$) (Figure 3.47.D.). This increase again began to have a tendency for reduction however, the significant increase remained (0.5 μM CBD, 1.98 ± 0.279 R.I., $p<0.05$; 1 μM CBD, 1.82 ± 0.257 R.I., $p<0.05$; 2.5 μM CBD, 1.42 ± 0.143 R.I., $p<0.05$; 5 μM CBD, 1.42 ± 0.143 R.I., $p<0.05$).

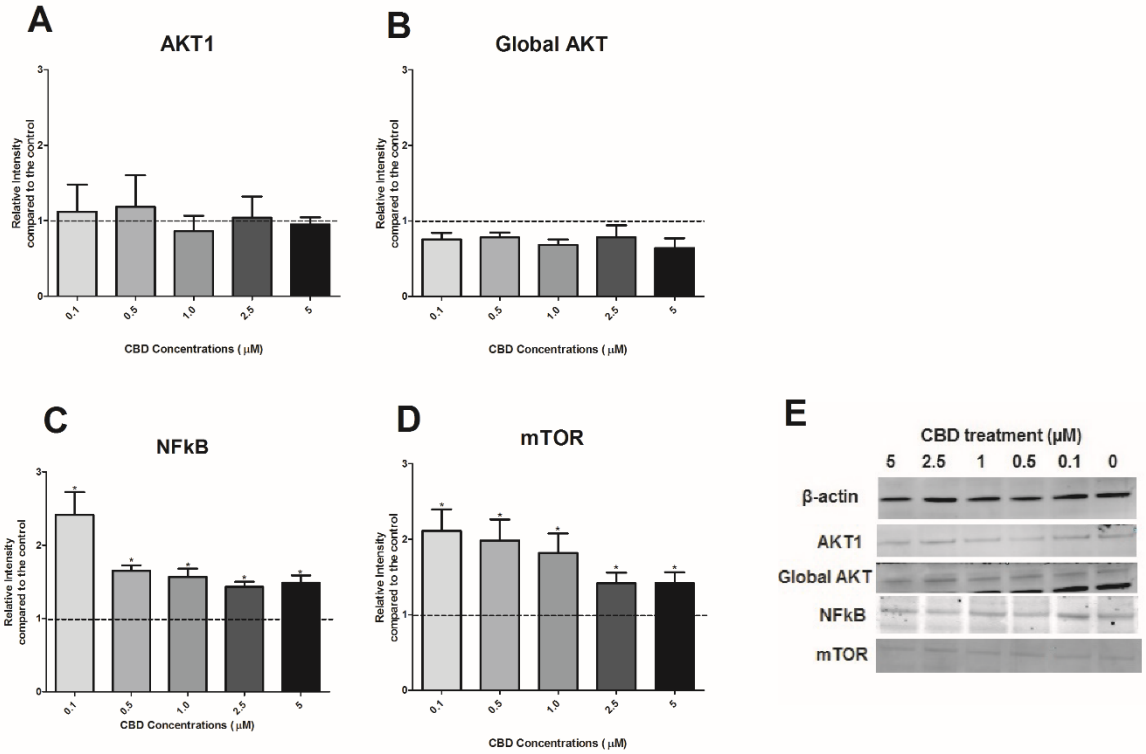

Figure 3.47. The chronic treatment of CBD's effect on protein levels in the AKT pathway in control cells.
Control cell's AKT pathway was examined after chronic CBD treatment. **(A)** AKT1, **(B)** Global AKT, **(C)** mTOR and **(D)** NFκB protein expression levels were examined compared to untreated cells with untreated (0) and the housekeeper β-actin as control protein. Data shown is repeated 3-5 times with the dashed line representing untreated levels. Data is represented as mean ± SEM. *$p<0.05$, **$p<0.01$, *** $p<0.001$ *vs* Untreated.

3.13. The chronic treatment of cells with CBD's effect on global DNA methylation state

3.13.1. The effect of global DNA methylation following chronic CBD treatment in cancer cells

The ratio of 5-methylCytosine to Guanine was assessed in order to ascertain potential changes in overall total methylation in each treatment group (Section 2.14.). Cancer cells showed no change in global methylation levels following chronic CBD treatment (Figure 3.48.).

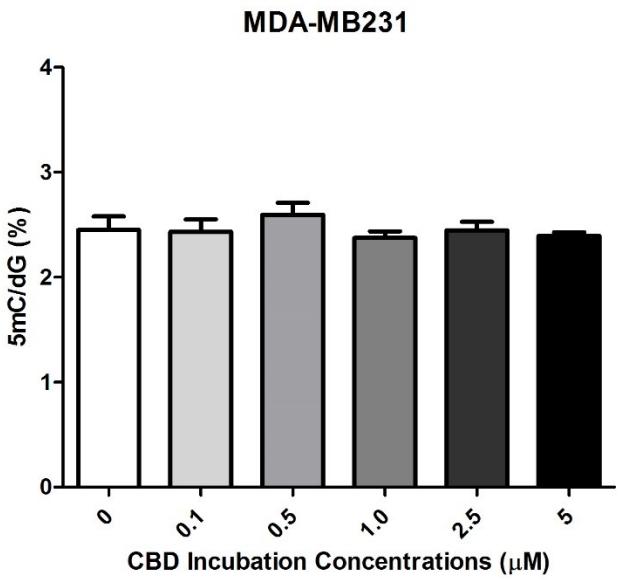

Figure 3.48. The effect of chronic CBD treatment on global DNA methylation state in cancer cells.
Cancer cells were treated with CBD for 24 hours and 5methylCytosine/dGuanine methylation levels were observed. Data shown is repeated 4 times with 2-3 technical replicates per run. Data is represented as mean ± SEM.

3.13.2. The effect of chronic CBD treatment on the global DNA methylation state of control cells

Following chronic CBD treatment the control cells were hypomethylated compared to untreated cells (Figure 3.49.). There was a significant reduction in methylation state following treatment with 0.1 μM CBD (2.77 ± 0.129 %) ($p<0.05$). This significant reduction remained constant as the dose of CBD increased (0.5 μM CBD,

2.69 ± 0.175 %, p<0.05; 1 μM CBD, 2.65 ± 0.169 %, p<0.05; 2.5 μM CBD, 2.76 ± 0.123 %, p<0.05; 5 μM CBD, 2.74 ± 0.129 %, p<0.05; untreated, 3.29 ± 0.265 %).

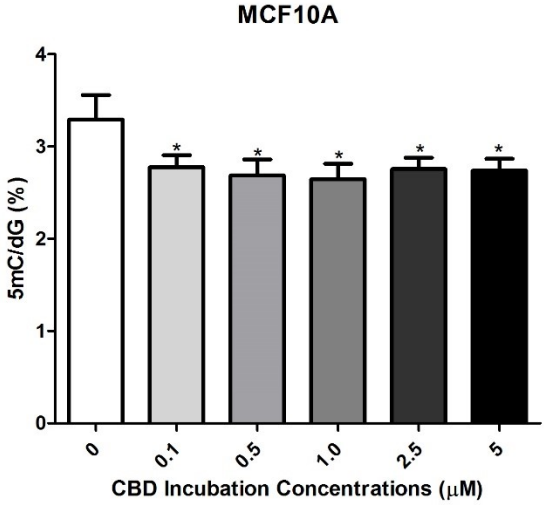

Figure 3.49. The effect of chronic CBD treatment on DNA methylation state in control cells.
Control cells, treated with CBD for 24 hours were analysed for differences in 5methylCytosine/dGuanine levels compared to untreated cells. Data shown is repeated 4 times with 2-3 technical replicates per plate. Data is represented as mean ± SEM. *p<0.05 *vs* untreated.

3.14. Summary following the treatment of CBD in both cancer and control cells

- **The optimal working conditions of CBD treatment**

Following a dose dependant examination an optimal working dose of 1 μM CBD was chosen which significantly reduced cancer cells ($p<0.001$) but not in control cells following 24 hours of treatment (Section 3.4.1. and 3.4.2.).

- **The mode of action of CBD in the cell**

The molecular mechanism of chronic CBD treatment was established to be through increased ROS and Ca^{2+} concentrations to levels that can induce cell death (Section 3.6. and 3.7.). In parallel an increase in VDAC1 activity was observed which is involved in increased apoptosis through increased cytochrome *c* release (Section 3.10.). Furthermore, following CBD treatment the cancer cells reversed the "Warburg Effect" with increased mitochondrial respiration and ATP levels suggesting mitochondrial dysfunction (Section 3.8.). Moreover, p53 and Nrf2 activity was increased while AKT levels were unchanged (Section 3.11. and 3.12.). This dual activation of p53 and Nrf2 showed that CBD activated a mild-stress response increasing cell death (Lau *et al.* 2008, Chen *et al.* 2012). Finally, this response to chronic CBD treatment was only observed in cancer cells and not in control cells. Control cells saw no change to cell viability, ROS concentration, VDAC1 activity or to its mitochondria.

- **The potential of CBD as a “priming” agent**

The potential of CBD as a “priming” agent was investigated in this study. “Priming” has been suggested to enhance chemotherapy’s activity through mitochondrial sensitisation (Chonghaile *et al.* 2011, Reed 2011, Sarosiek *et al.* 2013). Mitochondrial sensitisation was achieved with CBD through increased ROS and Ca^{2+} concentration in cancer cells. In parallel VDAC1 activity was increased while the mitochondrial function was dysregulated (Bragado *et al.* 2007, Koczor *et al.* 2013, Rimmerman *et al.* 2013, Sarosiek *et al.* 2013). Most importantly these alterations were only observed with 24 hours treatment of 1 μM CBD in cancer cells and not in control cells.